

# On the Validity of Modeling SGD with Stochastic Differential Equations (SDEs)

Zhiyuan Li<sup>1</sup> Sadhika Malladi<sup>1</sup> Sanjeev Arora<sup>1,2</sup>

## Abstract

It is generally recognized that finite learning rate (LR), in contrast to infinitesimal LR, is important for good generalization in real-life deep nets. Most attempted explanations propose approximating finite-LR SGD with Itô Stochastic Differential Equations (SDEs). But formal justification for this approximation (e.g., (Li et al., 2019a)) only applies to SGD with tiny LR. Experimental verification of the approximation appears computationally infeasible. The current paper clarifies the picture with the following contributions: (a) An efficient simulation algorithm SVAG that provably converges to the conventionally used Itô SDE approximation. (b) Experiments using this simulation to demonstrate that the previously proposed SDE approximation can meaningfully capture the training and generalization properties of common deep nets. (c) A provable and empirically testable necessary condition for the SDE approximation to hold and also its most famous implication, the linear scaling rule (Smith et al., 2020; Goyal et al., 2017). The analysis also gives rigorous insight into why the SDE approximation may fail.

## 1. Introduction

Training with Stochastic Gradient Descent (SGD) (1) and finite learning rate (LR) is largely considered essential for getting best performance out of deep nets: using infinitesimal LR (which turns the process into *Gradient Flow* (GF)) or finite LR with full gradient results in noticeably worse test error despite sometimes giving better training error (Wu et al., 2020; Smith et al., 2020; Bjorck et al., 2018).

Mathematical explorations of the implicit bias of finite-LR SGD toward good generalization have focused on the *noise* arising from gradients being estimated from small batches. This has motivated modeling SGD as a *stochastic process* and, in particular, studying Stochastic Differential Equations

<sup>1</sup>Department of Computer Science, Princeton University, NJ USA <sup>2</sup>Institute for Advanced Study, NJ USA. Correspondence to: Zhiyuan Li <zhiyuanli@cs.princeton.edu>.

(SDEs) to understand the evolution of net parameters.

Early attempts to analyze the effect of noise try to model it as a fixed Gaussian (Jastrzebski et al., 2017; Mandt et al., 2017). Current approaches approximate SGD using a parameter-dependent noise distribution that match the first and second order moments of the SGD (Equation (2)). It is important to realize that this approximation is *heuristic* for finite LR, meaning it is not known whether the two trajectories actually track each other closely. Experimental verification seems difficult because simulating the (continuous) SDE requires full gradient/noise computation over suitably fine time intervals. Recently, (Li et al., 2017; 2019a) provided a rigorous proof that the trajectories are arbitrarily close in a natural sense, but the proof needs the LR of SGD to be an unrealistically small (unspecified) constant so the approximation remains heuristic. An experimental study (Simsekli et al., 2019) suggested that the SDE approximation actually fails because the noise in gradient estimation is heavy tailed and not Gaussian, though followup work (Xie et al., 2021) points to flaws in that study.

Setting aside the issue of *correctness* of the SDE approximation, there is no doubt it has yielded important insights of practical importance, especially the *linear scaling rule* (LSR; see Definition 5.1) relating batch size and optimal LR, which allows much faster training using high parallelism (Krizhevsky, 2014; Goyal et al., 2017). However, since the scaling rule depends upon the validity of the SDE approximation, it is not mathematically understood when the rule fails. (Empirical investigation, with some intuition based upon analysis of simpler models, appears in (Smith et al., 2020; Goyal et al., 2017).)

This paper casts new light on the SDE approximation via the following contributions:

1. A new and efficient numerical method, *Stochastic Variance Amplified Gradient* (SVAG), to test if the trajectories of SGD and its corresponding SDE are close for a given model, dataset, and hyperparameter configuration. In Theorem 4.1, we prove (using ideas similar to (Li et al., 2019a)) that SVAG provides an order-1 weak approximation to the corresponding SDE. (Section 4)
2. Empirical testing showing that the trajectory under SVAG converges and closely follows SGD, suggesting (in combination with the previous result) that the SDE

approximation can be a meaningful approach to understanding the implicit bias of SGD in deep learning.

3. New theoretical insight into the observation in (Goyal et al., 2017; Smith et al., 2020) that linear scaling rule fails at large LR/batch sizes (Section 6). It applies to networks that use normalization layers (*scale-invariant* nets in (Arora et al., 2019b)), which includes most popular architectures. We give a necessary condition for the SDE approximation to hold: *at equilibrium, the gradient norm must be smaller than its variance*. This easily testable condition is rigorously proven and supersedes the previous intuitions of (Smith et al., 2020), which we point out are simplistic in light of the recent *edge of stability* phenomenon described in (Cohen et al., 2021).

## 2. Related Work

**Applications of the SDE approximation in deep learning.** One component of the SDE approximation is the gradient noise distribution. When the noise is an isotropic Gaussian distribution (i.e.,  $\Sigma(X_t) \equiv I$ ), then the equilibrium of the SDE is the Gibbs distribution. (Shi et al., 2020) used an isotropic Gaussian noise assumption to derive a convergence rate on SGD that clarifies the role of the LR during training. Several works have relaxed the isotropic assumption but assume the noise is constant. (Mandt et al., 2017) assumed the covariance  $\Sigma(X)$  is locally constant to show that SGD can be used to perform Bayesian posterior inference. (Zhu et al., 2019) argued that when constant but anisotropic SGD noise aligns with the Hessian of the loss, SGD is able to more effectively escape sharp minima.

Recently, many works have used the most common form of the SDE approximation (2) with parameter-dependent noise covariance. (Li et al., 2020) and (Kunin et al., 2020) used the symmetry of loss (scale invariance) to derive properties of dynamics (i.e.,  $\Sigma(X_t)X_t = 0$ ). (Li et al., 2020) further used this property to explain the phenomenon of sudden rising error after LR decay in training. (Smith et al., 2020) used the SDE to derive the linear scaling rule ((Goyal et al., 2017) and Definition 5.1) for infinitesimally small LR. (Xie et al., 2021) constructed a SDE-motivated diffusion model to propose why SGD favors flat minima during optimization. (Cheng et al., 2020) analyzed MCMC-like continuous dynamics and construct an algorithm that provably converges to this limit, although their dynamics do not model SGD.

Some works have challenged the traditional Gaussian noise assumption. (Simsekli et al., 2019; Nguyen et al., 2019) suggested that SGD noise is heavy-tailed, which (Zhou et al., 2020) claimed causes adaptive gradient methods to generalize better than SGD. However, (Xie et al., 2021) claimed that the measurements in (Simsekli et al., 2019) were flawed and argue that the noise may in fact be Gaussian.

**Theoretical Foundations of the SDE approximation for SGD.** Despite the popularity of using SDEs to study SGD, theoretical justification for this approximation has generally relied upon tiny LR (Li et al., 2019a; Hu et al., 2019). (Cheng et al., 2020) proved a strong approximation result for an SDE and MCMC-like dynamics, but not SGD. (Wu et al., 2020) argued that gradient descent with Gaussian noise can generalize as well as SGD, but their convergence proof also relied on an infinitesimally small LR.

**LR and Batch Size.** It is well known that using large batch size or small LR will lead to worse generalization (Bengio, 2012; LeCun et al., 2012). According to (Keskar et al., 2017), generalization is harmed by the tendency for large-batch training to converge to sharp minima, but (Dinh et al., 2017) argued that the invariance in ReLU networks can permit sharp minima to generalize well too. (Li et al., 2019b) argued that the LR can change the order in which patterns are learned in a non-homogeneous synthetic dataset. Several works (Hoffer et al., 2017; Smith & Le, 2018; Chaudhari & Soatto, 2018; Smith et al., 2018) have had success using a larger LR to preserve the scale of the gradient noise and hence maintain the generalization properties of small-batch training. The relationship between LR and generalization remains hazy, as (Shallue et al., 2019) empirically demonstrated that the generalization error can depend on many other training hyperparameters.

## 3. Notation and Preliminaries

**Notations:** We use  $|\cdot|$  to denote the  $\ell_2$  norm of a vector and  $\otimes$  to denote the tensor product.

Stochastic Gradient Descent (SGD) is often used to solve optimization problems of the form  $\min_{x \in \mathbb{R}^d} \mathcal{L}(x) := \mathbb{E}_\gamma \mathcal{L}_\gamma(x)$  where  $\{\mathcal{L}_\gamma : \gamma \in \Gamma\}$  is a family of functions from  $\mathbb{R}^d$  to  $\mathbb{R}$  and  $\gamma$  is a  $\Gamma$ -valued variable, e.g., denoting a random batch of training data. We consider the general case of an expectation over arbitrary index sets and distributions.

The *Stochastic Gradient Descent* (SGD) is defined as:

$$x_{k+1} = x_k - \eta \nabla \mathcal{L}_{\gamma_k}(x_k), \quad (1)$$

where each  $\gamma_k$  is an i.i.d. random variable with the same distribution as  $\gamma$ .

Past works used the following *canonical SDE approximation* for SGD (1), where  $X_t$  is the parameter vector at (continuous) time  $t$ ,  $W_t$  is white noise, and  $\Sigma(x_k) := \mathbb{E}[(\nabla \mathcal{L}_{\gamma_k}(x_k) - \nabla \mathcal{L}(x_k))(\nabla \mathcal{L}_{\gamma_k}(x_k) - \nabla \mathcal{L}(x_k))^\top | x_k]$ .

$$dX_t = -\nabla \mathcal{L}(X_t)dt + (\eta \Sigma(X_t))^{1/2}dW_t. \quad (2)$$

$\Sigma(x_k)$  is the covariance of the gradient, so it captures the gradient noise that comes from sampling a batch instead of performing full-batch gradient descent. We refer to this SDE as the Ito SDE, and when  $W_t$  is replaced by a Levy process (Definition A.1), we call the SDE a Levy SDE (8).

As mentioned, the approximation is heuristic. To understand whether two stochastic processes track each other closely, one must look at the distributions of outcomes (e.g., trained nets) they produce. Mathematics formulates closeness of distributions in terms of expectations of suitable classes of test functions<sup>1</sup>. Meaningful test functions in ML involve properties of trained nets such as train and test error, which do not satisfy formal conditions such as differentiability assumed in classical theory but can be still used in experiments (see Figures 1 and 2). In Section 6, we use another set of metrics including weight norm  $|x_t|$ , gradient norm  $|\nabla \mathcal{L}(x_t)|$  and trace of noise covariance  $\text{Tr}[\Sigma(x_t)]$  as the test functions and prove a sufficient condition for the failure of SDE approximation w.r.t. to this set of test functions.

**Definition 3.1** (Test Functions). Class  $G$  of continuous functions  $\mathbb{R}^d \rightarrow \mathbb{R}$  has *polynomial growth* if for every  $g \in G$  there exist positive integers  $\kappa_1, \kappa_2 > 0$  such that for all  $x \in \mathbb{R}^d$ ,  $|g(x)| \leq \kappa_1(1 + |x|^{2\kappa_2})$ .

For integer  $\alpha \geq 1$ , we denote by  $G^\alpha$  the set of  $\alpha$ -times continuously differentiable functions  $\mathbb{R}^d \rightarrow \mathbb{R}$  where partial derivatives of order  $\leq \alpha$ , i.e., all partial derivatives of form  $\frac{\partial^\alpha g}{\partial x_1^{\alpha_1} \dots \partial x_d^{\alpha_d}}$  s.t.  $\sum_{i=1}^d \alpha_i = \bar{\alpha} \leq \alpha$ , are also in  $G$ .

**Definition 3.2** (Order- $\alpha$  weak approximation). Let  $\{X_t^\eta : t \in [0, T]\}$  and  $\{x_k^\eta\}_{k=0}^{\lfloor \frac{T}{\eta} \rfloor}$  be families of continuous and discrete stochastic process parametrized by  $\eta$ . We say  $\{X_t^\eta\}$  and  $\{x_k^\eta\}$  are order- $\alpha$  weak approximations of each other if for every  $g \in G^\alpha$ , there is a constant  $C > 0$  independent of  $\eta$  such that

$$\max_{k=0, \dots, \lfloor \frac{T}{\eta} \rfloor} \left| \mathbb{E}g(x_k^\eta) - \mathbb{E}g(X_{k\eta}^\eta) \right| \leq C\eta^\alpha.$$

When applicable, we drop the superscript  $\eta$ , and say  $\{X_t\}$  and  $\{x_k\}$  are *order- $\alpha$  (or  $\alpha$  order) approximations* of each other.

The following is formal evidence of the goodness of the canonical approximation.

**Theorem 3.3** (Li et al., 2019a). *The SDE (2) is a first order weak approximation of SGD (1).*

## 4. Stochastic Variance Amplified Gradient (SVAG)

We provide an efficient algorithm, *Stochastic Variance Amplified Gradient* (SVAG), to approximate the corresponding Ito-SDE for a particular training setting. In Theorem 4.1, we prove that SVAG converges weakly to the SDE (2). Then, in Figures 1 and 2, we use SVAG to verify that training PreResNet-32 on CIFAR-10 using SGD can be accurately

<sup>1</sup>Test functions are reminiscent of GANs in machine learning, where the discriminator net can be viewed as a test function for the two distributions.

modeled using the Ito SDE approximation, and Appendix E contains additional settings. Hence, the contribution of SVAG is two-fold: first, it provides a computationally efficient way to simulate the SDE (2); second, it can be used to test if a given training setting is close to the SDE approximation.

### 4.1. The SVAG Algorithm

For a chosen hyperparameter  $l \in \mathbb{N}^+$ , we define

$$x_{k+1} = x_k - \frac{\eta}{l} \nabla \mathcal{L}_{\bar{\gamma}_k}^l(x_k), \quad (3)$$

where  $\bar{\gamma}_k = (\gamma_{k,1}, \gamma_{k,2})$  with  $\gamma_{k,1}, \gamma_{k,2}$  sampled independently and

$$\mathcal{L}_{\bar{\gamma}_k}^l(\cdot) := \frac{1 + \sqrt{2l - 1}}{2} \mathcal{L}_{\gamma_{k,1}}(\cdot) + \frac{1 - \sqrt{2l - 1}}{2} \mathcal{L}_{\gamma_{k,2}}(\cdot).$$

SVAG independently samples two batches  $\gamma_{k,1}$  and  $\gamma_{k,2}$  and computes the loss for each of them. Then, the loss is a linear combination of the individual losses, ensuring that the expected loss is preserved but multiplying the variance by a factor of  $l$ , i.e.,  $\sqrt{\frac{\eta}{l}} \Sigma^l(x) = \sqrt{\eta} \Sigma^1(x)$ , where  $\Sigma^l(x) := \mathbb{E}[(\nabla \mathcal{L}_{\bar{\gamma}_k}^l(x_k) - \nabla \mathcal{L}^l(x_k))(\nabla \mathcal{L}_{\bar{\gamma}_k}^l(x_k) - \nabla \mathcal{L}^l(x_k))^\top | x_k]$ . In this way, the Ito SDE that matches the first and second order moments is always (2). We note that SVAG is equivalent to SGD when  $l = 1$ , and when  $l$  increases, each step has smaller expectation but larger variance.

### 4.2. SVAG Approximates the SDE

We now show that SVAG converges weakly to the Ito SDE approximation in (2) when  $l \rightarrow \infty$ , i.e.,  $x_{lk}$  and  $X_{k\eta}$  have the roughly same distribution. Figures 1 and 2 provide verification of the below theorem, and additional settings are studied in Appendix E.

**Theorem 4.1.** *Suppose the following conditions<sup>2</sup> are met:*

- (i)  $\mathcal{L} \equiv \mathbb{E}\mathcal{L}_\gamma$  is  $\mathcal{C}^\infty$ -smooth, and  $\mathcal{L} \in G^4$ .
- (ii)  $|\nabla \mathcal{L}_\gamma(x) - \nabla \mathcal{L}_\gamma(y)| \leq L_\gamma |x - y|$ , for all  $x, y \in \mathbb{R}^d$ , where  $L_\gamma > 0$  is a random variable with finite moments, i.e.,  $\mathbb{E}L_\gamma^k$  is bounded for  $k \in \mathbb{N}^+$ .
- (iii)  $\Sigma^{\frac{1}{2}}(X)$  is  $\mathcal{C}^\infty$ -smooth in  $X$ .

Let  $T, \eta > 0$  be constants, and set  $N = \lfloor lT/\eta \rfloor$ , where  $l$  is the SVAG hyperparameter (3). Define  $\{X_t : t \in [0, T]\}$  as the stochastic process (independent of  $\eta$ ) satisfying the Ito SDE (2) and  $\{x_k^{\eta/l} : 1 \leq k \leq N\}$  as the trajectory of SVAG (3). Then, SVAG  $\{x_k^{\eta/l}\}$  is an order-1 weak approximation of the SDE  $\{X_t\}$ , i.e. for each  $g \in G^4$ , there exists a constant  $C > 0$  independent of  $l$  such that

$$\max_{k=0, \dots, N} |\mathbb{E}g(x_k^{\eta/l}) - \mathbb{E}g(X_{\frac{k\eta}{l}})| \leq Cl^{-1}.$$

<sup>2</sup>The  $\mathcal{C}^\infty$  smoothness assumptions can be relaxed by using the mollification technique in (Li et al., 2019a).

**Remark 4.2.** Lipschitz condition like (ii) are often not met by deep learning objectives. For instance using normalization schemes can make derivatives unbounded, but if trajectory of  $\{x_t\}$  stays bounded away from the origin and infinity, then (ii) holds.

The derivation is based on the following two-step process, following the agenda of (Li et al., 2019a):

1. Showing that the approximation error on a finite interval ( $N = \lfloor \frac{Tl}{\eta} \rfloor$  steps) can be upper bounded by the sum of expected one-step errors. (Theorem 4.3, which is Theorem 3 in (Li et al., 2019a))
2. Showing the one-step approximation error of SVAG is of order 2, and so the approximation on a finite interval is of order 1. (Lemmas 4.4 and 4.5)

### 4.3. Relating one-step to $N$ -step approximations

First, we show that we can construct an approximation over a finite interval by building a one-step approximation. Let  $T, l > 0$  be constants, and define  $N = \lfloor lT/\eta \rfloor$ , where  $l$  is the SVAG hyperparameter (3). For convenience, we also define  $\tilde{X}_k := X_{\frac{k\eta}{l}}$ . Further, let  $\{X_t^{x,s} : t \geq s\}$  denote the stochastic process obeying the Ito SDE (2) with the initial condition  $X_s^{x,s} = x$ . We similarly write  $\tilde{X}_k^{x,j} := X_{\frac{k\eta}{l}}^{x,\frac{j\eta}{l}}$  and denote by  $\{x_k^{x,j} : k \geq j\}$  the stochastic process (depending on  $l$ ) satisfying SVAG (3) but with  $x_j^{x,j} = x$ . Alternatively, we write  $\tilde{X}_k(x, j) := \tilde{X}_k^{x,j}$  and  $x_k(x, j) := x_k^{x,j}$ . By definition,  $\tilde{X}_k(x_k, k) = x_k$  and  $\tilde{X}_k(x_0, 0) = \tilde{X}_k$ .

Thus we have for any  $1 \leq k \leq \lfloor \frac{lT}{\eta} \rfloor$ ,

$$\begin{aligned} |\mathbb{E}g(x_k) - \mathbb{E}g(X_{\frac{k\eta}{l}})| &= |\mathbb{E}g(x_k) - \mathbb{E}g(\tilde{X}_k)| \\ &\leq \sum_{j=0}^{k-1} |\mathbb{E}g(\tilde{X}_k(x_{j+1}, j+1)) - \mathbb{E}g(\tilde{X}_k(x_j, j))| \\ &= \sum_{j=0}^{k-1} |\mathbb{E}u^{k,j+1}(\tilde{X}_{j+1}(x_j, j)) - \mathbb{E}u^{k,j+1}(x_{j+1}(x_j, j))| \\ &= \sum_{j=0}^{k-1} |\mathbb{E}u^{k,j+1}(\tilde{X}_1(x_j, 0)) - \mathbb{E}u^{k,j+1}(x_1(x_j, 0))| \end{aligned}$$

where  $u^{k,j+1}(x)$  is defined as  $\mathbb{E}g(\tilde{X}_k(x, j+1))$  and the last step is because of SDE (2) is time-homogeneous.

Now it's clear that if the one step change of SVAG and SDE, which are  $\Delta(x_j)$  and  $\tilde{\Delta}(x_j)$  defined below, are  $O(\frac{\eta^2}{l^2})$ -close in distribution conditioned on every  $x_j$ , then after  $\lfloor \frac{lT}{\eta} \rfloor$  steps the error is at most  $O(\frac{l}{\eta})$ .

$$\Delta(x) := x_1^{x,0} - x, \quad \tilde{\Delta}(x) := \tilde{X}_1^{x,0} - x. \quad (4)$$

The above analysis can be formally stated by the following theorem, adapted from (Li et al., 2019a) to our setting. For completeness, we provide its proof in Appendix B.1.

**Theorem 4.3** (Adaption of Theorem 3 in (Li et al., 2019a)). Let  $T > 0$  and  $N = \lfloor lT/\eta \rfloor$ . Suppose further that the following conditions hold:

- (i) There is a function  $K_1 \in G$  independent of  $l$  such that  $|\mathbb{E}\Delta(x)^{\otimes s} - \mathbb{E}\tilde{\Delta}(x)^{\otimes s}| \leq K_1(x)l^{-2}$  for  $s = 1, 2, 3$  and  $\sqrt{\mathbb{E}|\Delta(x)^{\otimes 4}|^2} \leq K_1(x)l^{-2}$ .
- (ii) For each  $m \geq 1$ , the  $2m$ -moment of  $x_k^{x,0}$  is uniformly bounded with respect to  $k$  and  $l$ , i.e. there exists a  $K_2 \in G$ , independent of  $l, k$ , such that  $\mathbb{E}|x_k^{x,0}|^{2m} \leq K_2(x)$ , for all  $k = 0, \dots, N \equiv \lfloor lT/\eta \rfloor$ .

Then, for each  $g \in G^4$ , there exists a constant  $C > 0$ , independent of  $l$ , such that

$$\max_{k=0, \dots, N} |\mathbb{E}g(x_k) - \mathbb{E}g(X_{\frac{k\eta}{l}})| \leq Cl^{-2}$$

### 4.4. One-step approximation

Below we will show the one step error between  $\Delta(x)$  and  $\tilde{\Delta}(x)$  is  $O(l^{-2})$ , which guarantees (i) in Theorem 4.3. Combining Lemma C.3 which proves (ii) in Theorem 4.3, we've proved the Theorem 4.1 by Theorem 4.3.

**Lemma 4.4.** Let  $\tilde{\Delta}(x)$  be defined as in (20). Then we have

- (i)  $\mathbb{E}\tilde{\Delta}(x) = \frac{\eta}{l}\nabla\mathcal{L}(x) + \mathcal{O}(l^{-2})$ ,
- (ii)  $\mathbb{E}\tilde{\Delta}(x)\tilde{\Delta}(x)^\top = \frac{\eta^2}{l}\Sigma(x) + \mathcal{O}(l^{-2})$ ,
- (iii)  $\mathbb{E}\tilde{\Delta}(x)^{\otimes 3} = \mathcal{O}(l^{-2})$ ,
- (iv)  $\sqrt{\mathbb{E}|\Delta(x)^{\otimes 4}|^2} = \mathcal{O}(l^{-2})$ .

Next, we estimate the moments of the SVAG iterations. (iii) and (iv) below are the main places that the properties of SVAG got used. It's worth noting that, though (i) and (ii) hold for any discrete iterations with  $LR = \frac{\eta}{l}$  and matching first and second order moments to SDE (2), (iii) and (iv) could fail, e.g., decreasing LR along with using a smaller batch size. (See a more detailed discussion in Section 5.2)

**Lemma 4.5.** Let  $\Delta(x)$  be defined as in (20) with the SVAG iterations, we have

- (i)  $\mathbb{E}\Delta(x) = -\nabla\mathcal{L}(x)\frac{\eta}{l}$ ,
- (ii)  $\mathbb{E}\Delta(x)\Delta(x)^\top = \frac{\eta^2}{l}\Sigma(x) + \frac{\eta^2}{l^2}\nabla\mathcal{L}(x)\nabla\mathcal{L}(x)^\top$ ,
- (iii)  $\mathbb{E}\Delta(x)^{\otimes 3} = \frac{\eta^3}{l^2}\frac{3-l^{-1}}{2}\Lambda(x) + \frac{\eta^3}{l^3}\left(3\overline{\nabla\mathcal{L}(x) \otimes \Sigma(x)} + \nabla\mathcal{L}(x)^{\otimes 3}\right)$
- (iv)  $\sqrt{\mathbb{E}|\Delta(x)^{\otimes 4}|^2} = \mathcal{O}(l^{-2})$ ,

where  $\Lambda(x) := \mathbb{E}(\nabla\mathcal{L}_{\gamma_1}(x) - \nabla\mathcal{L}(x))^{\otimes 3}$ , and  $\overline{\mathcal{T}}$  denotes the symmetrization of tensor  $\mathcal{T}$ , i.e.,  $\overline{\mathcal{T}}_{ijk} = \frac{1}{6}\sum_{i',j',k'} \mathcal{T}_{i'j'k'}$ , where  $i', j', k'$  is a permutation of  $i, j, k$ .

## 5. Two Failure Modes of SDE Approximation

In this section, we diagnose two ways in which the SDE (2) may fail to approximate finite LR SGD: *discretization error*

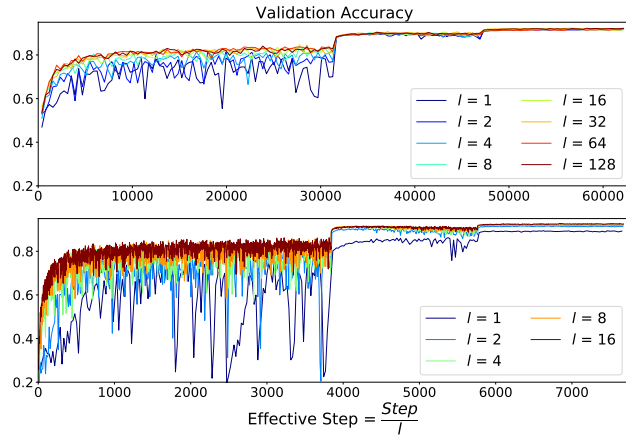


Figure 1. Validation accuracy for PreResNet-32 during training on CIFAR-10 using  $B = 64$ ,  $LR = 0.8$  (top) and  $B = 1024$ ,  $LR = 6.4$  (bottom). LR is decayed by 0.1 at epoch 80 and 120 in both baselines. For standard setting ( $B = 64$ ), SVAG achieves similar performance for all  $l$ , suggesting SDE (2) is a valid approximation. While for large batch size ( $B = 1024$ ), SVAG outperforms SGD starting from  $l = 2$ , showing that the large-batch SGD could not be well approximated by SDE (2). We investigate this failure further in Section 6. Since SVAG takes  $l$  smaller steps to simulate the continuous dynamics in  $\eta$  time, we plot accuracy against “effective steps” defined as  $\frac{\# \text{steps}}{l}$ .

and *non-Gaussian noise*. To distinguish these failure modes, we define the following variant of SGD, *Noisy Gradient Descent*, which replaces SGD noise at each step by a multivariate Gaussian random variable with equal covariance. The notion of NGD also appeared in (Wu et al., 2020).

#### Noisy Gradient Descent (NGD):

$$\hat{x}_{k+1} = \hat{x}_k - \eta \nabla \mathcal{L}(\hat{x}_k) + \Sigma^{\frac{1}{2}}(\hat{x}_k) z_k, \quad (5)$$

where  $z_k \stackrel{\text{i.i.d.}}{\sim} N(0, I_d)$ ,  $\forall k \in \mathbb{N}$ .

We then define the following **Error Decomposition**:

$$\begin{aligned} & \mathbb{E}g(X_{\eta k}) - \mathbb{E}g(x_k) \\ &= \underbrace{(\mathbb{E}g(X_{\eta k})) - \mathbb{E}g(\hat{x}_k)}_{\text{Discretization Error}} + \underbrace{(\mathbb{E}g(\hat{x}_k)) - \mathbb{E}g(x_k)}_{\text{Gap by non-Gaussian noise}} \end{aligned} \quad (6)$$

Applying Theorem 4.1 to the original SGD (1) and NGD (5) reveals that SVAG simultaneously causes the discretization error and the gap between the original non-Gaussian noise and white noise to disappear. (See a more detailed explanation in Section 5.2) From Figure 1, we can observe that for vision tasks, the test accuracy of deep nets trained by SGD in the standard settings stays the same when interpolating towards SDE via SVAG, suggesting that neither the non-Gaussian nature of SGD noise nor the discrete nature of SGD dynamics is an essential ingredient of the generalization mystery of deep learning.

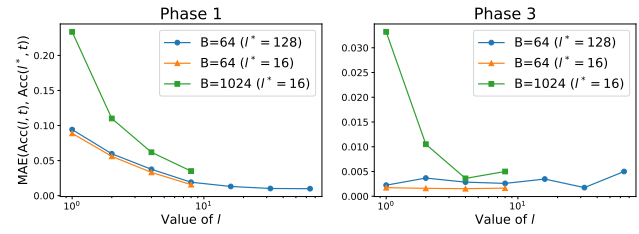


Figure 2. SVAG converges in terms of test accuracy w. both large and small batch size. Interestingly, for  $B = 64$ , even SGD is outperformed by SVAG in the phase 1 (see Figure 1), they end up to be very close in phase 3. We define the MAE of test accuracy between SVAG with  $l$  and  $l^*$  (both with batch size  $B$ ) in phase  $i$  the by  $\sum_{t=T_{i-1}}^{T_i-1} |\text{Acc}(t, l) - \text{Acc}(t, l^*)| / (T_i - T_{i-1})$ , where  $T_{i-1}$  is the starting epoch of phase  $i$ .

#### 5.1. Large LR and discretization error

The first term in (6), *discretization error*, is defined as the gap between SDE (2) and SGD (1) caused by large LR. If we scrutinize the proof of Lemma 4.4, we can also write the second-order Taylor expansion for  $\mathbb{E}\tilde{\Delta}(x)$  as

$$\mathbb{E}\tilde{\Delta}(x) = \frac{\eta}{l} \nabla \mathcal{L}(x) + \frac{\eta^2}{2l^2} \nabla^2 \mathcal{L}(x) \nabla \mathcal{L}(x) + \mathcal{O}(l^{-3}).$$

As such, discretization error can occur even without stochasticity or noise, e.g., full-batch GD diverges from Gradient Flow (GF) when LR becomes too large (Figure 3). In the case of full-batch GD, when LR is only moderately small, the second-order term above is too large to be ignored so the training dynamics are sensitive to LR. It's also known that GD with moderately small LR can find solutions of different quality than GF. For example, Cohen et al. (2021) showed that full-batch GD with modern deep nets usually operate at the “edge of the stability” and the sharpness of the learnt solution, i.e., the largest eigenvalue of the hessian, depends on the learning rate.

However, SGD dynamics are not necessarily sensitive to LR when the noise dominates the gradient, e.g. following the famous *Linear Scaling Rule* (LSR, Definition 5.1), SGD with larger batch size and LR can achieve similar performance.

**Definition 5.1** (Linear Scaling Rule). (Krizhevsky, 2014; Goyal et al., 2017) For  $\kappa > 0$ , when the minibatch size is multiplied by  $\kappa$ , multiply the LR by  $\kappa$ .

(Smith et al., 2020) defined the *noise dominated regime* as the setting in which noise dominates the gradient and the *curvature dominated regime* as the setting in which SGD behaves similarly to full-batch GD. They showed experimentally that in noise dominated regime, the training properties, including the optimal LR, are controlled by noise.

In Section 6 we provide a more mathematically rigorous condition for the curvature dominated regime of deep nets with normalization layers, using the ratio between expected gradient and noise as a measurement. We show the SDE

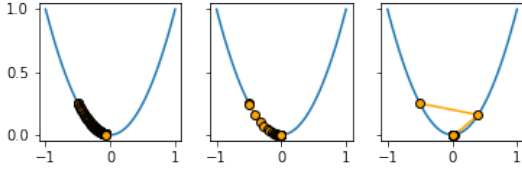


Figure 3. From left to right, gradient descent on  $f(x) = x^2$  with  $\eta = 1e-3$ ,  $\eta = 0.01$ , and  $\eta = 0.9$ . As  $\eta$  increases, the discretization error increases.

approximation provably breaks when the magnitude of the expected gradient exceeds that of the noise, regardless of the shape of the noise distribution. Furthermore, the reason that the SDE approximation breaks is exactly that second order term in  $\mathbb{E}\Delta(x)$  cannot be ignored in this case. We also found a novel necessary condition for the LSR to hold using this insight.

## 5.2. Non-Gaussian noise

To understand the second failure mode caused by non-Gaussian noise, for convenience we assume the noise is infinitely divisible, below. That is, for the original SGD (1), for any  $m \in \mathbb{N}^+$ , there is a random loss function  $\mathcal{L}_{\gamma^m}$ , such that for any  $x \in \mathbb{R}^d$ , the original stochastic gradient  $\nabla\mathcal{L}_{\gamma}(x)$  could be simulated by the sum of  $m$  i.i.d. sampled stochastic gradients  $\nabla\mathcal{L}_{\gamma_i^m}(x)$ , for  $i = 1, \dots, m$ :

$$\nabla\mathcal{L}_{\gamma}(x) \stackrel{d}{=} \sum_{i=1}^m \nabla\mathcal{L}_{\gamma_i^m}(x). \quad (7)$$

For SGD with batch size  $B$ , such a random loss function can be found when  $m$  is a factor of  $B$ , in which case it suffices to define  $\mathcal{L}^m$  as the product of  $\frac{m}{B}$  and the same loss function with a smaller batch size  $\frac{B}{m}$ .<sup>3</sup> It's well known that every infinitely divisible distribution corresponds to a Levy process (Definition A.1)  $Z(t) \in \mathbb{R}^d$ , in the sense that  $\nabla\mathcal{L}_{\gamma}(x) \stackrel{d}{=} Z(1)$  (Ken-Iti, 1999). If we further assume there is a Levy process  $Z(t)$  and a function  $\sigma(x) : \mathbb{R}^d \rightarrow \mathbb{R}^{d \times d}$  such that for every  $x$ ,  $\nabla\mathcal{L}_{\gamma}(x) - \nabla\mathcal{L}(x) \stackrel{d}{=} \sigma(x)Z(1)$ , then by Theorem 2.2 in (Protter et al., 1997), SGD will converge to a limiting continuous dynamic, which we denote as the *Levy SDE*, as the LR decreases to 0 along LSR. Formally,  $\sigma$  is the solution of the following SDE driven by a Levy process.

$$dX_t = -\eta \nabla\mathcal{L}(X_t) + \sqrt{\eta} \sigma(X_t) dZ_t \quad (8)$$

In the special case where  $Z_t$  is the  $d$ -dimensional Brownian motion,  $\sigma(x)$  will be the square root of the noise covariance,  $\Sigma^{\frac{1}{2}}(x)$ . The Levy SDE is equal to the limit of SVAG, (i.e., the Ito SDE) only when the noise is strictly Gaussian. Thus

<sup>3</sup>Batch loss of nets with BatchNorm is not necessarily divisible, because (7) doesn't hold, as the individual loss depends on the entire batch of data with the presence of BN. Still, it holds for ghost BatchNorm (Hoffer et al., 2017) with  $B$  equal to the number of mini-ghost batches.

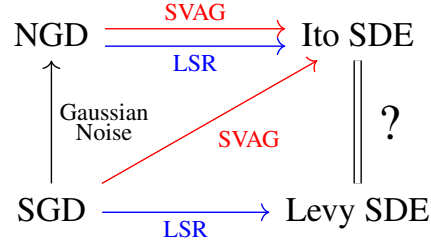


Figure 4. Relationship between SGD, NGD, Ito SDE and Levy SDE. Here we assume the noise in SGD is infinitely divisible such that the LR can go to 0 along LSR. For NGD, i.e., SGD with Gaussian noise, both SVAG and LSR (Linear Scaling Rule) approaches the same continuous limit. This does not hold for SGD with non-Gaussian noise.

the gap induced by non-Gaussian noise will not vanish even if both SGD and NGD decrease the LR along LSR, as it will converge to the gap between Ito SDE and Levy SDE. See Figure 4 for a summary of the relationships among SGD, NGD, Ito SDE, and Levy SDE.

We also note that though (Smith et al., 2020) derives LSR by assuming the Ito SDE approximation holds, this is only a sufficient but not necessary condition for LSR. In Section F.1, we provide a concrete example where LSR holds for all LRs and batch sizes, but the dynamic is constantly away from Ito SDE limit. In particular, the discretization error can disappear even with constant LR as long as the the loss landscape and noise distribution are smooth enough (or more extremely, gradient and noise distribution being parameter-independent).

Since LSR converges to a different limit than SVAG does, it's natural to ask which part of the approximation in Lemma 4.5 fails. By scrutinizing the proof of Lemma 4.5, we can see (i) and (ii) still hold for any stochastic discrete process with LR  $\frac{\eta}{l}$  and matching first and second order moments, while the term  $\frac{\eta^3(3-l^{-1})}{2l^2} \Lambda(x)$  now becomes  $\frac{\eta^3}{l} \Lambda(x)$  for SGD along LSR, which is larger by an order of  $l$ . Therefore, the single-step approximation error becomes  $O(l^{-1})$  and the total error after  $\lfloor Tl/\eta \rfloor$  steps remains constant.<sup>4</sup>

**How does GD with Gaussian noise perform in practice?** As mentioned before, the fact that SVAG achieves the same test accuracy suggests the generalization magic of SGD is not necessarily related to the specific shape of its noise beyond the covariance when LR vanishes. So how does GD with Gaussian noise of same covariance perform with finite LR? Interestingly, although a priori the learned solutions could come from very different distributions, in Figure 5, we found that the training/test curves are still close for wide PreResNet32 trained on CIFAR-10. Similar experiments were conducted in (Wu et al., 2020) but used SGD with momentum. These findings confirm the conclusion

<sup>4</sup>Such error does not only occur in the third order moment. It also appears in the higher moments. Therefore simply assuming the noise distribution is symmetric (thus  $\Lambda = 0$ ) won't fix this gap.

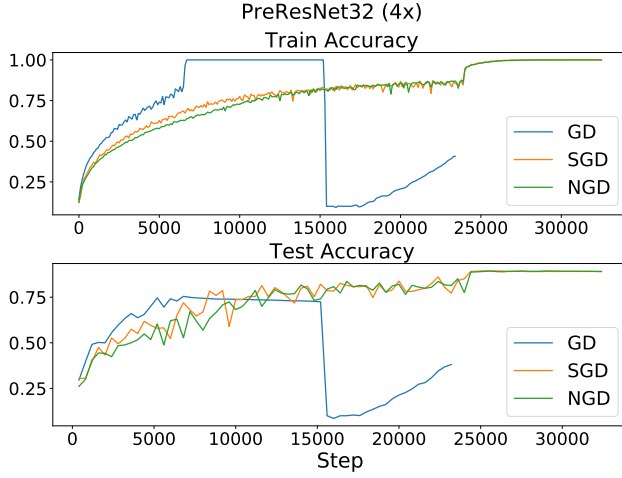


Figure 5. SGD and NGD with matching covariance have close train (top) and test (bottom) curves. The batch size for SGD is 125 and LR = 0.8 for all three settings and decayed by 0.1 at step 24000. GD achieves 75.5% test accuracy, and SGD and NGD achieve 89.4% and 89.3%, respectively. We smooth the training curve by dividing it into intervals of 100 steps and recording the average. For efficient sampling of Gaussian noise, we use GroupNorm instead of BatchNorm and turn off data augmentation. See implementation details in Appendix E.

in (Cheng et al., 2020) that differences in the third-and-higher moments in SGD noise don't affect the test accuracy significantly, though differences in the second moments do.

## 6. Provable Failure of SDE Approximation and Linear Scaling Rule with Large LR

In this section, we provide a sufficient condition on LR to answer the following question for normalized networks (e.g. BatchNorm (Ioffe & Szegedy, 2015) and GroupNorm (Wu & He, 2018)) trained by SGD + Weight Decay (WD): *Given a fixed SDE (9), when does SGD (10) with matching moments have a very different equilibrium?*

$$dX_t = -\nabla(\mathcal{L}(X_t) + \frac{\lambda}{2}|X_t|^2)dt + \Sigma^{1/2}(X_t)dW_t \quad (9)$$

The moment-matching SGD (10) satisfies  $\mathcal{L}(x) = \mathbb{E}\mathcal{L}_\gamma(x)$  and  $\eta\Sigma(x)$  is the covariance of  $\nabla\mathcal{L}_\gamma(x)$ .

$$x_{k+1} = x_k - \eta\nabla(\mathcal{L}_{\gamma_k}(x_k) + \frac{\lambda}{2}|x_k|^2) \quad (10)$$

First we want to clarify what we mean by being *very different*. Ideally, we should measure the similarity in terms of train/test loss or accuracy, but the optimization and generalization for deep nets beyond NTK regime (Jacot et al., 2018; Allen-Zhu et al., 2019b; Du et al., 2019; Zou et al., 2020; Arora et al., 2019a; Allen-Zhu et al., 2019a) is in general still an open problem. Here we will propose the following criterion involving three basic metrics: squared weight norm  $|x|^2$ , squared gradient norm  $|\nabla\mathcal{L}(x)|^2$  and trace of

noise covariance,  $\text{Tr}[\Sigma(x)]$ . One would expect that if the two trajectories reach different equilibria, then one of these metrics will differ by a multiplicative constant.

**Definition 6.1** ( $C$ -closeness). We use

$$R_\infty := \lim_{t \rightarrow \infty} \mathbb{E}|x_t|^2, \quad \bar{R}_\infty := \lim_{t \rightarrow \infty} \mathbb{E}|X_t|^2,$$

$$G_\infty := \lim_{t \rightarrow \infty} \mathbb{E}|\nabla\mathcal{L}(x_t)|^2, \quad \bar{G}_\infty := \lim_{t \rightarrow \infty} \mathbb{E}|\nabla\mathcal{L}(X_t)|^2,$$

$$N_\infty := \lim_{t \rightarrow \infty} \mathbb{E}[\text{Tr}[\Sigma(x_t)]], \quad \bar{N}_\infty := \lim_{t \rightarrow \infty} \mathbb{E}[\text{Tr}[\Sigma(X_t)]]$$

to denote the limiting squared norm, gradient norm and trace of covariance for SGD (10) and the corresponding limits for SDE (9). (We assume both  $x_t$  and  $X_t$  converge to their equilibrium so the limits exist). We say the two equilibria are  $C$ -close to each other iff

$$\frac{1}{C} \leq \frac{R_\infty}{\bar{R}_\infty}, \frac{G_\infty}{\bar{G}_\infty}, \frac{\eta N_\infty}{\bar{N}_\infty} \leq C. \quad (11)$$

Now we will show formally how the above defined  $C$ -closeness will break for large LR.

**Theorem 6.2.** *If the equilibria of (10) and (9) exist and are  $C$ -close, then  $\eta \leq \frac{\bar{N}_\infty}{G_\infty}(C^2 - 1)$ .*

A key point is that for normalized networks, the so-called scale-invariance property (Arora et al., 2019b) holds, implying that  $\mathcal{L}_\gamma(x) = \mathcal{L}_\gamma(cx)$ , for any  $c > 0$  and  $x \in \mathbb{R}^d$ . By the chain rule, we have  $\langle \nabla\mathcal{L}_\gamma(x), x \rangle = 0$  for every  $x \in \mathbb{R}^d$ . Following the derivation in (Li et al., 2020), we have

$$\frac{d}{dt}|X_t|^2 = -2\lambda|X_t|^2 + \text{Tr}[\Sigma(X_t)]. \quad (12)$$

It can be shown that for SGD (10), it holds that

$$\begin{aligned} & \mathbb{E}|x_{k+1}|^2 - \mathbb{E}|x_k|^2 \\ &= (1 - \eta\lambda)^2 \mathbb{E}|x_k|^2 + \eta^2 \mathbb{E}|\nabla\mathcal{L}(X_t)|^2 - \mathbb{E}|x_k|^2 \\ &= \eta\lambda(-2 + \eta\lambda) \mathbb{E}|x_k|^2 + \eta^2 \mathbb{E}|\nabla\mathcal{L}(x_k)|^2 + \eta^2 \mathbb{E} \text{Tr}[\Sigma(x_k)] \end{aligned} \quad (13)$$

If both  $x_k$  and  $X_t$  have reached their equilibria, then the LHS of (12) and (13) are both 0, and therefore

$$(2 - \eta\lambda)\lambda R_\infty = \eta G_\infty + \eta N_\infty, \quad (14)$$

$$2\lambda \bar{R}_\infty = \quad + \bar{N}_\infty. \quad (15)$$

By combining (14), (15), and (11), we have

$$\eta G_\infty + \eta N_\infty \leq 2\lambda R_\infty \leq 2\lambda C \bar{R}_\infty = C \bar{N}_\infty.$$

Applying (11) again, we have

$$\eta \bar{G}_\infty + \bar{N}_\infty \leq C\eta(G_\infty + N_\infty) \leq C^2 \bar{N}_\infty.$$

In other words, whenever  $\eta > \frac{\bar{N}_\infty}{G_\infty}(C^2 - 1)$ , regardless of the shape (i.e., the third-and-higher moments) of the noise,

## On the Validity of Modeling SGD with SDEs

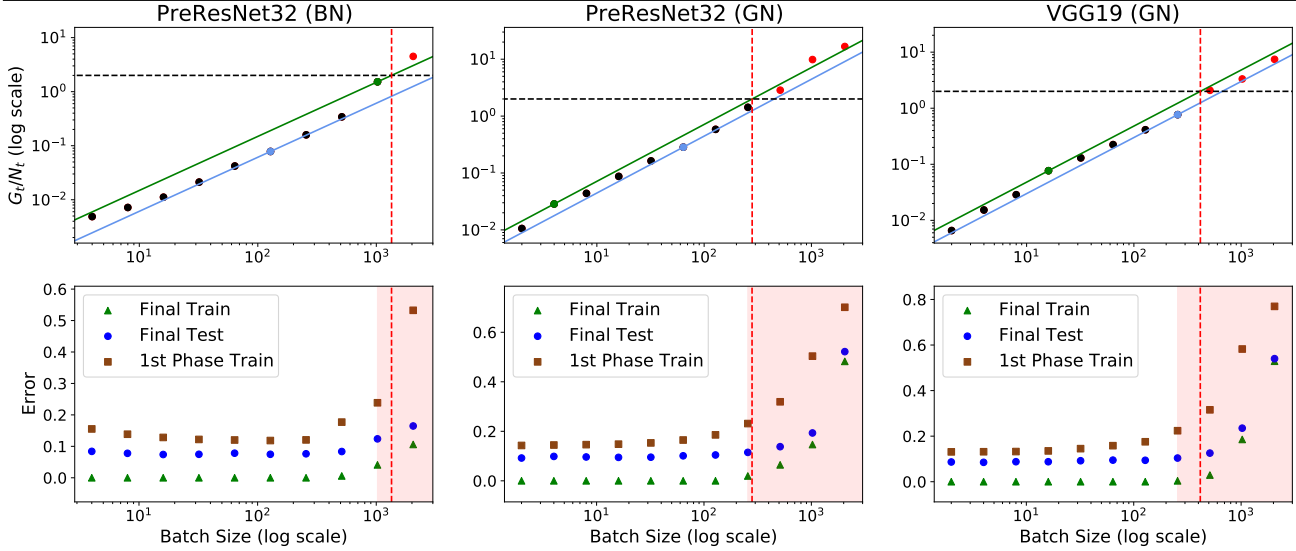


Figure 6. Experimental verification for our theory on predicting the failure of Linear Scaling Rule. We modify PreResNet-32 and VGG-19 to be scale-invariant (According to Appendix C of (Li et al., 2020)). All three settings use the same lr schedule,  $LR = 0.8$  initially and is decayed by 0.1 at epoch 250 with 300 epochs total budget. Here,  $G_t$  and  $N_t$  are the empirical estimations of  $G_\infty$  and  $N_\infty$  taken after reaching equilibrium in the first phase (before LR decay). Per the approximated version of Theorem 6.6, i.e.,  $B^* = \kappa B \lesssim C^2 B N_\infty^B / G_\infty^B$ , we use baseline runs with different batch sizes  $B$  to report the maximal and minimal predicted critical batch size, defined as the intersection of the threshold ( $G_t/N_t = C^2$ ) with the green and blue lines, respectively. We choose a threshold of  $C^2 = 2$ , and consider LSR to fail if the final test error exceeds the lowest achieved test error by more than 20% of its value, marked by the red region on the plot. Surprisingly, it turns out the condition in Theorem 6.6 is not only necessary, but also close to sufficient. Further settings and discussion is in Appendix E.

the equilibrium of SGD (10) won't be  $C$ -close to the equilibrium of SDE (9). In particular, the SDE (9) misses the term of  $\eta G_\infty$  because it is a second order term in the one-step error. This gap can also be found between SDE and other continuous dynamics that are order-2 weak approximations for SGD, e.g., the *Stochastic Modified Equation* in (Li et al., 2019a). In Appendix D, we show the equilibrium of 2nd order SDE approximation (16) cannot be  $C$ -close to that of 1st order SDE approximation (2) for large LR.

**Theorem 6.3** (2nd Order SDE Approximation). (Li et al., 2019a) (16) is a 2nd order weak approximation of SGD (1):

$$\begin{aligned} dX_t = & -\eta \nabla (\mathcal{L}(X_t) + \frac{\eta}{4} \|\nabla \mathcal{L}(X_t)\|_2^2) dt \\ & + \sqrt{\eta} (\Sigma(X_t))^{1/2} dW_t \end{aligned} \quad (16)$$

We can also use  $\eta \geq \frac{N_\infty}{G_\infty} (C^2 - 1)$  as a more formal definition for the curvature dominated regime proposed in (Smith et al., 2020) for normalized networks. The original definition in (Smith et al., 2020) of the critical LR  $\epsilon_{crit} := 2/\lambda_{max}$  is somewhat circular: to know whether a single run with LR  $\eta$  belongs to the curvature dominated regime (i.e., if  $\eta$  is larger than  $\epsilon_{crit}$ ), one must first evaluate the  $\lambda_{max}$ , the largest eigenvalue of the Hessian of the local convex approximation of the loss. Hence,  $\lambda_{max}$  depends on the trajectory of SGD, and thus the LR  $\eta$  itself! As pointed out by (Cohen et al., 2021), the smoothness along the trajectory depends heavily on the chosen LR. Compared to

the original definition, the new threshold  $\frac{N_\infty}{G_\infty} (C^2 - 1)$  is well-defined and provides the desired guarantee that LSR induced by successful SDE approximation will break when LR exceeds this threshold.

Still, there are two pitfalls: first,  $\frac{N_\infty}{G_\infty}$  cannot be measured as simulating the SDE with high precision is computationally expensive; second, in practice, people are often more interested in how closely the performance of large batch SGD matches that of its small batch counterpart, instead of how closely it matches the SDE limit. We address these issues below by adapting the analysis above to understand LSR.

### 6.1. Provable Failure of Linear Scaling Rule

In this section we derive a necessary condition for LSR to hold for finite LR. As above, we will use  $R_\infty^B, G_\infty^B, N_\infty^B$  to denote the limiting squared norm, gradient norm and trace of covariance for SGD (10) with LR  $= \frac{\eta}{B}$  and  $\mathcal{L}_\gamma$  as a i.i.d. sampled stochastic loss with mini-batch of size  $B$ . We first introduce the concept of Linear Scaling Invariance (LSI):

**Definition 6.4** (( $C, \kappa$ )-Linear Scaling Invariance). We say SGD (10) with batch size  $B$  exhibits  $(C, \kappa)$ -LSI if, for a constant  $C$  such that  $0 < C < \sqrt{\kappa}$ ,

$$\frac{1}{C} \leq \frac{R_\infty^B}{R_\infty^{\kappa B}}, \frac{N_\infty^B}{\kappa N_\infty^{\kappa B}}, \frac{G_\infty^B}{G_\infty^{\kappa B}} \leq C. \quad (17)$$

We show below that  $(C, \kappa)$ -LSI fails if  $\frac{G_\infty^{\kappa B}}{N_\infty^{\kappa B}}$  is larger than

some setting-dependent constant.

**Theorem 6.5.** Assuming  $(C, \kappa)$ -LSI, regardless of the value of  $R_\infty^B, G_\infty^B, N_\infty^B$ , it holds that

$$\frac{N_\infty^{\kappa B}}{G_\infty^{\kappa B}} \geq \frac{1}{C^2} - \frac{1}{\kappa} \quad (18)$$

In other words, this theorem gives us a certificate for failure of  $(C, \kappa)$ -LSI without even running the baseline. Interestingly, the following theorem shows we can also predict the largest batch size for which  $(C, \kappa)$ -LSI holds just with a single run of baseline:

**Theorem 6.6.** Assuming  $(C, \kappa)$ -LSI holds, we have

$$\kappa \leq C^2 \left(1 + \frac{N_\infty^B}{G_\infty^B}\right), \quad (\approx C^2 \frac{N_\infty^B}{G_\infty^B} \text{ when } \frac{N_\infty^B}{G_\infty^B} \gg 1).$$

## 7. Conclusion

We present a computationally efficient simulation SVAG (Section 4) that provably converges to the canonical 1st order SDE (2), which we use to verify that the SDE is a meaningful approximation for SGD in common deep learning settings. In Section 5, we then discuss two reasons the SDE approximation may fail to approximate finite LR SGD: discretization error and non-Gaussian noise. We relate the discretization error to LSR (Definition 5.1): in Section 6 we derive a testable necessary condition for the SDE approximation (and thus, LSR) to hold, and in Figure 6 we demonstrate its applicability to standard settings.

## References

Allen-Zhu, Z., Li, Y., and Liang, Y. Learning and generalization in overparameterized neural networks, going beyond two layers. In *Advances in Neural Information Processing Systems*, volume 32. Curran Associates, Inc., 2019a. URL <https://proceedings.neurips.cc/paper/2019/file/62dad6e273d32235ae02b7d321578ee8-Paper.pdf>.

Allen-Zhu, Z., Li, Y., and Song, Z. A convergence theory for deep learning via over-parameterization. In Chaudhuri, K. and Salakhutdinov, R. (eds.), *Proceedings of the 36th International Conference on Machine Learning*, volume 97 of *Proceedings of Machine Learning Research*, pp. 242–252, Long Beach, California, USA, 09–15 Jun 2019b. PMLR.

Arora, S., Du, S., Hu, W., Li, Z., and Wang, R. Fine-grained analysis of optimization and generalization for overparameterized two-layer neural networks. In *International Conference on Machine Learning*, pp. 322–332. PMLR, 2019a.

Arora, S., Li, Z., and Lyu, K. Theoretical analysis of auto-rate-tuning by batch normalization. In *International Conference on Learning Representations*, 2019b.

Bengio, Y. Practical recommendations for gradient-based training of deep architectures. In *Neural networks: Tricks of the trade*, pp. 437–478. Springer, 2012.

Biewald, L. Experiment tracking with weights and biases, 2020. URL <https://www.wandb.com/>. Software available from wandb.com.

Bjorck, N., Gomes, C. P., Selman, B., and Weinberger, K. Q. Understanding batch normalization. In Bengio, S., Wallach, H., Larochelle, H., Grauman, K., Cesa-Bianchi, N., and Garnett, R. (eds.), *Advances in Neural Information Processing Systems 31*, pp. 7694–7705. Curran Associates, Inc., 2018.

Chaudhari, P. and Soatto, S. Stochastic gradient descent performs variational inference, converges to limit cycles for deep networks. In *International Conference on Learning Representations*, 2018.

Cheng, X., Yin, D., Bartlett, P., and Jordan, M. Stochastic gradient and langevin processes. In *International Conference on Machine Learning*, pp. 1810–1819. PMLR, 2020.

Cohen, J., Kaur, S., Li, Y., Kolter, J. Z., and Talwalkar, A. Gradient descent on neural networks typically occurs at the edge of stability. In *International Conference on Learning Representations*, 2021. URL <https://openreview.net/forum?id=jh-rTtvkGeM>.

Dinh, L., Pascanu, R., Bengio, S., and Bengio, Y. Sharp minima can generalize for deep nets. In *Proceedings of the 34th International Conference on Machine Learning-Volume 70*, pp. 1019–1028. JMLR.org, 2017.

Du, S. S., Zhai, X., Poczos, B., and Singh, A. Gradient descent provably optimizes over-parameterized neural networks. In *International Conference on Learning Representations*, 2019.

Goyal, P., Dollár, P., Girshick, R., Noordhuis, P., Wesolowski, L., Kyrola, A., Tulloch, A., Jia, Y., and He, K. Accurate, large minibatch sgd: Training imagenet in 1 hour. *arXiv preprint arXiv:1706.02677*, 2017.

He, K., Zhang, X., Ren, S., and Sun, J. Deep residual learning for image recognition. In *Proceedings of the IEEE conference on computer vision and pattern recognition*, pp. 770–778, 2016.

Hoffer, E., Hubara, I., and Soudry, D. Train longer, generalize better: closing the generalization gap in large batch training of neural networks. In Guyon, I., Luxburg, U. V.,

Bengio, S., Wallach, H., Fergus, R., Vishwanathan, S., and Garnett, R. (eds.), *Advances in Neural Information Processing Systems 30*, pp. 1731–1741. Curran Associates, Inc., 2017.

Hoffer, E., Hubara, I., and Soudry, D. Fix your classifier: the marginal value of training the last weight layer. In *International Conference on Learning Representations*, 2018.

Hu, W., Li, C. J., Li, L., and Liu, J.-G. On the diffusion approximation of nonconvex stochastic gradient descent. *Annals of Mathematical Sciences and Applications*, 4(1), 2019.

Ioffe, S. and Szegedy, C. Batch normalization: accelerating deep network training by reducing internal covariate shift. In *Proceedings of the 32nd International Conference on International Conference on Machine Learning-Volume 37*, pp. 448–456. JMLR. org, 2015.

Jacot, A., Gabriel, F., and Hongler, C. Neural tangent kernel: Convergence and generalization in neural networks. In Bengio, S., Wallach, H., Larochelle, H., Grauman, K., Cesa-Bianchi, N., and Garnett, R. (eds.), *Advances in Neural Information Processing Systems 31*, pp. 8571–8580. Curran Associates, Inc., 2018.

Jastrzebski, S., Kenton, Z., Arpit, D., Ballas, N., Fischer, A., Bengio, Y., and Storkey, A. Three factors influencing minima in sgd. *arXiv preprint arXiv:1711.04623*, 2017.

Ken-Iti, S. *Lévy processes and infinitely divisible distributions*. Cambridge university press, 1999.

Keskar, N. S., Mudigere, D., Nocedal, J., Smelyanskiy, M., and Tang, P. T. P. On large-batch training for deep learning: Generalization gap and sharp minima. In *International Conference on Learning Representations*, 2017.

Krizhevsky, A. One weird trick for parallelizing convolutional neural networks. *arXiv preprint arXiv:1404.5997*, 2014.

Kunin, D., Sagastuy-Brena, J., Ganguli, S., Yamins, D. L. K., and Tanaka, H. Neural mechanics: Symmetry and broken conservation laws in deep learning dynamics, 2020. URL <https://arxiv.org/pdf/2012.04728v1.pdf>.

LeCun, Y. A., Bottou, L., Orr, G. B., and Müller, K.-R. *Efficient BackProp*, pp. 9–48. Springer Berlin Heidelberg, Berlin, Heidelberg, 2012. ISBN 978-3-642-35289-8. doi: 10.1007/978-3-642-35289-8\_3.

Li, Q., Tai, C., and Weinan, E. Stochastic modified equations and adaptive stochastic gradient algorithms. In *Proceedings of the 34th International Conference on Machine Learning-Volume 70*, pp. 2101–2110. JMLR. org, 2017.

Li, Q., Tai, C., and Weinan, E. Stochastic modified equations and dynamics of stochastic gradient algorithms i: Mathematical foundations. *J. Mach. Learn. Res.*, 20:40–1, 2019a.

Li, Y., Wei, C., and Ma, T. Towards explaining the regularization effect of initial large learning rate in training neural networks. In Wallach, H., Larochelle, H., Beygelzimer, A., d’ Alché-Buc, F., Fox, E., and Garnett, R. (eds.), *Advances in Neural Information Processing Systems 32*, pp. 11674–11685. Curran Associates, Inc., 2019b.

Li, Z. and Arora, S. An exponential learning rate schedule for deep learning. In *International Conference on Learning Representations*, 2020.

Li, Z., Lyu, K., and Arora, S. Reconciling modern deep learning with traditional optimization analyses: The intrinsic learning rate. In Larochelle, H., Ranzato, M., Hadsell, R., Balcan, M., and Lin, H. (eds.), *Advances in Neural Information Processing Systems 33: Annual Conference on Neural Information Processing Systems 2020, NeurIPS 2020, December 6-12, 2020, virtual*, 2020. URL <https://proceedings.neurips.cc/paper/2020/hash/a7453a5f026fb6831d68bdc9cb0edcae-Abstract.html>.

Loshchilov, I. and Hutter, F. Sgdr: Stochastic gradient descent with warm restarts. *arXiv preprint arXiv:1608.03983*, 2016.

Mandt, S., Hoffman, M. D., and Blei, D. M. Stochastic gradient descent as approximate bayesian inference. *The Journal of Machine Learning Research*, 18(1):4873–4907, 2017.

Mohammadi, M., Mohammadpour, A., and Ogata, H. On estimating the tail index and the spectral measure of multivariate  $\alpha$ -stable distributions. *Metrika*, 78(5):549–561, 2015.

Netzer, Y., Wang, T., Coates, A., Bissacco, A., Wu, B., and Ng, A. Y. Reading digits in natural images with unsupervised feature learning. 2011.

Nguyen, T. H., Simsekli, U., Gürbüzbalaban, M., and Richard, G. First exit time analysis of stochastic gradient descent under heavy-tailed gradient noise. In Wallach, H. M., Larochelle, H., Beygelzimer, A., d’Alché-Buc, F., Fox, E. B., and Garnett, R. (eds.), *Advances in Neural Information Processing Systems 32: Annual Conference on Neural Information Processing Systems 2019, NeurIPS*

2019, December 8-14, 2019, Vancouver, BC, Canada, pp. 273–283, 2019. URL <https://proceedings.neurips.cc/paper/2019/hash/a97da629b098b75c294dffdc3e463904-Abstract.html>.

Protter, P., Talay, D., et al. The euler scheme for lévy driven stochastic differential equations. *The Annals of Probability*, 25(1):393–423, 1997.

Shallue, C. J., Lee, J., Antognini, J., Sohl-Dickstein, J., Frostig, R., and Dahl, G. E. Measuring the effects of data parallelism on neural network training. *Journal of Machine Learning Research*, 20(112):1–49, 2019. URL <http://jmlr.org/papers/v20/18-789.html>.

Shi, B., Su, W. J., and Jordan, M. I. On learning rates and schrödinger operators. *arXiv preprint arXiv:2004.06977*, 2020.

Simsekli, U., Sagun, L., and Gurbuzbalaban, M. A tail-index analysis of stochastic gradient noise in deep neural networks. In Chaudhuri, K. and Salakhutdinov, R. (eds.), *Proceedings of the 36th International Conference on Machine Learning*, volume 97 of *Proceedings of Machine Learning Research*, pp. 5827–5837. PMLR, 09–15 Jun 2019. URL <http://proceedings.mlr.press/v97/simsekli19a.html>.

Smith, L. N. Cyclical learning rates for training neural networks. In *2017 IEEE Winter Conference on Applications of Computer Vision (WACV)*, pp. 464–472, 2017. doi: 10.1109/WACV.2017.58.

Smith, S. L. and Le, Q. V. A bayesian perspective on generalization and stochastic gradient descent. In *International Conference on Learning Representations*, 2018.

Smith, S. L., Kindermans, P.-J., and Le, Q. V. Don’t decay the learning rate, increase the batch size. In *International Conference on Learning Representations*, 2018.

Smith, S. L., Elsen, E., and De, S. On the generalization benefit of noise in stochastic gradient descent, 2020.

Wu, J., Hu, W., Xiong, H., Huan, J., Braverman, V., and Zhu, Z. On the noisy gradient descent that generalizes as SGD. In III, H. D. and Singh, A. (eds.), *Proceedings of the 37th International Conference on Machine Learning*, volume 119 of *Proceedings of Machine Learning Research*, pp. 10367–10376, 13–18 Jul 2020.

Wu, Y. and He, K. Group normalization. *arXiv preprint arXiv:1803.08494*, 2018.

Xie, Z., Sato, I., and Sugiyama, M. A diffusion theory for deep learning dynamics: Stochastic gradient descent exponentially favors flat minima, 2021.

Zhang, J., Karimireddy, S. P., Veit, A., Kim, S., Reddi, S. J., Kumar, S., and Sra, S. Why are adaptive methods good for attention models? *arXiv preprint arXiv:1912.03194*, 2019.

Zhou, P., Feng, J., Ma, C., Xiong, C., HOI, S., and E, W. Towards theoretically understanding why sgd generalizes better than adam in deep learning, 2020.

Zhu, Z., Wu, J., Yu, B., Wu, L., and Ma, J. The anisotropic noise in stochastic gradient descent: Its behavior of escaping from sharp minima and regularization effects. In Chaudhuri, K. and Salakhutdinov, R. (eds.), *Proceedings of the 36th International Conference on Machine Learning*, volume 97 of *Proceedings of Machine Learning Research*, pp. 7654–7663. PMLR, 09–15 Jun 2019.

Zou, D., Cao, Y., Zhou, D., and Gu, Q. Gradient descent optimizes over-parameterized deep relu networks. *Machine Learning*, 109(3):467–492, 2020.

## A. Preliminary on Lévy Process

**Definition A.1.** We call a stochastic process  $X = \{X_t : t \geq 0\}$  a Levy process if it satisfies the following properties:

- $X_0 = 0$  almost surely;
- Independence of increments: For any  $0 \leq t_1 < t_2 < \dots < t_n < \infty$ ,  $X_{t_2} - X_{t_1}, X_{t_3} - X_{t_2}, \dots, X_{t_n} - X_{t_{n-1}}$  are independent;
- Stationary increments: For any  $s < t$ ,  $X_t - X_s$  is equal in distribution to  $X_{t-s}$ ;
- Continuity in probability: For any  $\varepsilon > 0$  and  $t \geq 0$  it holds that  $\lim_{h \rightarrow 0} P(|X_{t+h} - X_t| > \varepsilon) = 0$ .

## B. Omitted Derivation in Section 4

### B.1. Relating one-step to $N$ -step approximations

Let us consider generally the question of the relationship between one-step approximations and approximations on a finite interval. Let  $T > 0$  and  $N = \lfloor lT/\eta \rfloor$ . Let us also denote for convenience  $\tilde{X}_k := X_{\frac{k\eta}{l}}$ . Further, let  $\{X_t^{x,s} : t \geq s\}$  denote the stochastic process obeying the same Equation (2), but with the initial condition  $X_s^{x,s} = x$ . We similarly write  $\tilde{X}_k^{x,j} := X_{\frac{k\eta}{l}}^{x,\frac{j\eta}{l}}$  and denote by  $\{x_k^{x,j} : k \geq j\}$  the stochastic process (depending on  $l$ ) satisfying Equation (3) but with  $x_j = x$ .

Now, let us denote the one-step changes

$$\Delta(x) := x_1^{x,0} - x, \quad \tilde{\Delta}(x) := \tilde{X}_1^{x,0} - x. \quad (19)$$

The following result is the adapted from (Li et al., 2019a) to our setting, which relates one-step approximations with approximations on a finite time interval.

**Theorem 4.3** (Adaption of Theorem 3 in (Li et al., 2019a)). *Let  $T > 0$  and  $N = \lfloor lT/\eta \rfloor$ . Suppose further that the following conditions hold:*

- (i) *There is a function  $K_1 \in G$  independent of  $l$  such that  $|\mathbb{E}\Delta(x)^{\otimes s} - \mathbb{E}\tilde{\Delta}(x)^{\otimes s}| \leq K_1(x)l^{-2}$  for  $s = 1, 2, 3$  and  $\sqrt{\mathbb{E}|\Delta(x)^{\otimes 4}|^2} \leq K_1(x)l^{-2}$ .*
- (ii) *For each  $m \geq 1$ , the  $2m$ -moment of  $x_k^{x,0}$  is uniformly bounded with respect to  $k$  and  $l$ , i.e. there exists a  $K_2 \in G$ , independent of  $l, k$ , such that  $\mathbb{E}|x_k^{x,0}|^{2m} \leq K_2(x)$ , for all  $k = 0, \dots, N \equiv \lfloor lT/\eta \rfloor$ .*

*Then, for each  $g \in G^4$ , there exists a constant  $C > 0$ , independent of  $l$ , such that*

$$\max_{k=0, \dots, N} |\mathbb{E}g(x_k) - \mathbb{E}g(X_{\frac{k\eta}{l}})| \leq Cl^{-2}$$

*Proof of Theorem 4.3.* Let  $T, l > 0$ ,  $N = \lfloor lT/\eta \rfloor$  and for convenience we also define  $\tilde{X}_k := X_{\frac{k\eta}{l}}$ . Further, let  $\{X_t^{x,s} : t \geq s\}$  denote the stochastic process obeying the same Equation (2), but with the initial condition  $X_s^{x,s} = x$ . We similarly write  $\tilde{X}_k^{x,j} := X_{\frac{k\eta}{l}}^{x,\frac{j\eta}{l}}$  and denote by  $\{x_k^{x,j} : k \geq j\}$  the stochastic process (depending on  $l$ ) satisfying Equation (3) but with  $x_j = x$ . Alternatively, we write  $\tilde{X}_k(x, j) := \tilde{X}_k^{x,j}$  and  $x_k(x, j) := x_k^{x,j}$ . By definition,  $\tilde{X}_k(x_k, k) = x_k$  and  $\tilde{X}_k(x_0, 0) = \tilde{X}_k$ .

Thus we have for any  $1 \leq k \leq \lfloor \frac{lT}{\eta} \rfloor$ ,

$$\begin{aligned}
 |\mathbb{E}g(x_k) - \mathbb{E}g(X_{\frac{k\eta}{l}})| &= |\mathbb{E}g(x_k) - \mathbb{E}g(\tilde{X}_k)| \\
 &\leq \sum_{j=0}^{k-1} \left| \mathbb{E}g(\tilde{X}_k(x_{j+1}, j+1)) - \mathbb{E}g(\tilde{X}_k(x_j, j)) \right| \\
 &\leq \sum_{j=0}^{k-1} \left| \mathbb{E}g(\tilde{X}_k(x_{j+1}, j+1)) - \mathbb{E}g(\tilde{X}_k(x_j, j)) \right| \\
 &\leq \sum_{j=0}^{k-1} \left| \mathbb{E}u^{k,j+1}(\tilde{X}_{j+1}(x_j, j)) - \mathbb{E}u^{k,j+1}(x_{j+1}(x_j, j)) \right| \\
 &\leq \sum_{j=0}^{k-1} \left| \mathbb{E}u^{k,j+1}(\tilde{X}_1(x_j, 0)) - \mathbb{E}u^{k,j+1}(x_1(x_j, 0)) \right| \\
 &\leq \sum_{j=0}^{k-1} \mathbb{E} \left[ \left| \mathbb{E}u^{k,j+1}(\tilde{X}_1(x_j, 0)) - \mathbb{E}u^{k,j+1}(x_1(x_j, 0)) \right| \mid x_j \right],
 \end{aligned}$$

where  $u^{k,j+1}(x)$  is defined as  $\mathbb{E}g(X_k(x, j+1))$  and the second to the last step is because of SDE (2) is time-homogeneous. By Proposition 25 in (Li et al., 2019a),  $u^{k,j+1} \in G^4$  uniformly, thus by Lemma B.1, we know there exists  $K(x) = \kappa_1(1 + |x|^{2\kappa_2}) \in G$  such that

$$|\mathbb{E}g(x_k) - \mathbb{E}g(X_{\frac{k\eta}{l}})| \leq \sum_{j=0}^{k-1} \mathbb{E} [K(x_j)l^{-2}] \leq \sum_{j=0}^{k-1} \mathbb{E} [\kappa_1(1 + |x_j|^{2\kappa_2})l^{-2}]$$

By assumption (ii), we know the there is some  $K' \in G$ ,

$$|\mathbb{E}g(x_k) - \mathbb{E}g(X_{\frac{k\eta}{l}})| \leq \sum_{j=0}^{k-1} \mathbb{E} [\kappa_1(1 + |x_j|^{2\kappa_2})l^{-2}] \leq \sum_{j=0}^{\lfloor \frac{lT}{\eta} \rfloor - 1} \mathbb{E} [\kappa_1(1 + |x_j|^{2\kappa_2})l^{-2}] \leq K'(x)l^{-1},$$

which completes the proof.  $\square$

Recall that

$$\Delta(x) := x_1^{x,0} - x, \quad \tilde{\Delta}(x) := \tilde{X}_1^{x,0} - x. \quad (20)$$

**Lemma B.1.** Suppose  $u^1, \dots, u^k \in G^4$  uniformly, that is,  $u^1, \dots, u^k \in G$  and there's a single  $K_0 \in G$  such that  $\left| \frac{\partial^s u}{\partial x_{(i_1), \dots, x_{(i_j)}}}(x) \right| \leq K_0(x)$ , for  $s = 1, 2, 3, 4$  and  $i_j \in \{1, 2, \dots, d\}, j \in \{1, \dots, s\}$ . Let assumption (i),(ii) in Thm. 4.3 hold and  $K_1(x), K_2(x)$  be such functions. Then, there exists some  $K \in G$ , independent of  $l, r$ , such that

$$\left| \mathbb{E}u^r(x_1^{x,0}) - \mathbb{E}u^r(\tilde{X}_1^{x,0}) \right| \leq K(x)l^{-2}$$

*Proof.* W.L.O.G, we can assume  $K_0(x) = \kappa_{0,1}(1 + |x|^{2\kappa_{0,2}}) \leq K_0(x)^2$ , for  $\kappa_{0,1} > 0, \kappa_{0,2} \in \mathbb{N}^+$ , thus for  $\alpha \in [0, 1]$  and  $x, y \in \mathbb{R}^d$ , we have  $K_0((1 - \alpha)x + \alpha y) \leq \max(K_0(x), K_0(y)) \leq K_0(x) + K_0(y)$ . We also assume  $\mathbb{E}K_0(x_1^{x,0})^2 \leq K_0^2(x)$ .

Using Taylor's theorem with the Lagrange form of the remainder, we have for any  $j \in \{1, \dots, k\}$ ,

$$\begin{aligned} u^r(x_1^{x,0}) - u^r(\tilde{X}_1^{x,0}) &= \sum_{s=1}^3 \frac{1}{s!} \sum_{i_1, \dots, i_s=1}^d \prod_{j=1}^s [\Delta_{(i_j)}(x) - \tilde{\Delta}_{(i_j)}(x)] \frac{\partial^s u^r}{\partial x_{(i_1)}, \dots, x_{(i_j)}}(x) \\ &\quad + \frac{1}{4!} \sum_{i_1, \dots, i_4=1}^d \left[ \frac{\partial^4 u^r}{\partial x_{(i_1)}, \dots, x_{(i_4)}}(x + a\Delta(x)) \prod_{j=1}^4 \Delta_{(i_j)}(x) \right] \\ &\quad - \frac{1}{4!} \sum_{i_1, \dots, i_4=1}^d \left[ \frac{\partial^4 u^r}{\partial x_{(i_1)}, \dots, x_{(i_4)}}(x + a\Delta(x)) \prod_{j=1}^4 \Delta_{(i_j)}(x) \right] \end{aligned}$$

where  $a, \tilde{a} \in [0, 1]$ .

Taking expectations over the first term, using assumption (i) of Thm. B.1, we get

$$\left| \mathbb{E} \left[ \sum_{s=1}^3 \frac{1}{s!} \sum_{i_1, \dots, i_s=1}^d \prod_{j=1}^s [\Delta_{(i_j)}(x) - \tilde{\Delta}_{(i_j)}(x)] \frac{\partial^s u^r}{\partial x_{(i_1)}, \dots, x_{(i_j)}}(x) \right] \right| \leq l^{-2} \left( \frac{d}{1!} + \frac{d^2}{2!} + \frac{d^3}{3!} \right) K_1(x) K_0(x)$$

Taking expectations over the second term, using assumption (i) of Appendix B.1 and Lemma C.1, we get

$$\begin{aligned} &\left| \mathbb{E} \left[ \frac{1}{4!} \sum_{i_1, \dots, i_4=1}^d \left[ \frac{\partial^4 u^r}{\partial x_{(i_1)}, \dots, x_{(i_4)}}(x + a\Delta(x)) \prod_{j=1}^4 \Delta_{(i_j)}(x) \right] \right] \right| \\ &\leq \frac{1}{4!} \sum_{i_1, \dots, i_4=1}^d \mathbb{E} \left| \frac{\partial^4 u^r}{\partial x_{(i_1)}, \dots, x_{(i_4)}}(x + a\Delta(x)) \right| \left| \prod_{j=1}^4 \Delta_{(i_j)}(x) \right| \\ &\leq \frac{1}{4!} \sum_{i_1, \dots, i_4=1}^d \sqrt{\mathbb{E} \left| \frac{\partial^{(\alpha+1)} u^r}{\partial x_{(i_1)}, \dots, x_{(i_4)}}(x + a\Delta(x)) \right|^2 \mathbb{E} \left| \prod_{j=1}^4 \Delta_{(i_j)}(x) \right|^2} \\ &\leq \frac{1}{4!l^2} \sum_{i_1, \dots, i_4=1}^d \sqrt{\mathbb{E} \left| K_0(x) + K_0(x_1^{x,0}) \right|^2 K_1(x)^2} \end{aligned}$$

Note that by assumption (ii) of Appendix B.1, we have

$$\mathbb{E} \left| K_0(x) + K_0(x_1^{x,0}) \right|^2 \leq 2K_0(x)^2 + 2\mathbb{E} K_0(x_1^{x,0})^2 \leq 2K_0(x)^2 + 2K_2(x)^2 \leq (2K_0(x) + 2K_2(x))^2.$$

Thus,

$$\begin{aligned} &\left| \mathbb{E} \left[ \frac{1}{4!} \sum_{i_1, \dots, i_4=1}^d \left[ \frac{\partial^4 u^r}{\partial x_{(i_1)}, \dots, x_{(i_4)}}(x + a\Delta(x)) \prod_{j=1}^4 \Delta_{(i_j)}(x) \right] \right] \right| \\ &\leq l^{-2} \frac{d^4}{4!} (2K_0(x) + 2K_2(x)) K_1(x) \end{aligned}$$

We can deal with the third term similarly to the second term and thus we conclude

$$|\mathbb{E} u(x_1^{x,0}) - \mathbb{E} u(\tilde{X}_1^{x,0})| \leq K(x) l^{-2}$$

□

## B.2. One-step approximation

**Lemma 4.4.** Let  $\tilde{\Delta}(x)$  be defined as in (20). Then we have

- (i)  $\mathbb{E}\tilde{\Delta}(x) = \frac{\eta}{l}\nabla\mathcal{L}(x) + \mathcal{O}(l^{-2})$ ,
- (ii)  $\mathbb{E}\tilde{\Delta}(x)\tilde{\Delta}(x)^\top = \frac{\eta^2}{l}\Sigma(x) + \mathcal{O}(l^{-2})$ ,
- (iii)  $\mathbb{E}\Delta(x)^{\otimes 3} = \mathcal{O}(l^{-2})$ ,
- (iv)  $\sqrt{\mathbb{E}|\Delta(x)^{\otimes 4}|^2} = \mathcal{O}(l^{-2})$ .

*Proof.* To obtain (i)-(iii), we simply apply Lem. C.2 with  $\psi(z) = \prod_{j=1}^s (z_{(i_j)} - x_{(i_j)})$  for  $s = 1, 2, 3$  and  $i_j \in \{1, \dots, d\}$  respectively. (iv) is due to Lemma C.1.  $\square$

Next, we estimate the moments of the SVAG iterations below.

**Lemma 4.5.** Let  $\Delta(x)$  be defined as in (20) with the SVAG iterations, we have

- (i)  $\mathbb{E}\Delta(x) = -\nabla\mathcal{L}(x)\frac{\eta}{l}$ ,
- (ii)  $\mathbb{E}\Delta(x)\Delta(x)^\top = \frac{\eta^2}{l}\Sigma(x) + \frac{\eta^2}{l^2}\nabla\mathcal{L}(x)\nabla\mathcal{L}(x)^\top$ ,
- (iii)  $\mathbb{E}\Delta(x)^{\otimes 3} = \frac{\eta^3}{l^2} \frac{3-l^{-1}}{2} \Lambda(x)$   
 $\quad + \frac{\eta^3}{l^3} \left( 3\overline{\nabla\mathcal{L}(x) \otimes \Sigma(x)} + \nabla\mathcal{L}(x)^{\otimes 3} \right)$
- (iv)  $\sqrt{\mathbb{E}|\Delta(x)^{\otimes 4}|^2} = \mathcal{O}(l^{-2})$ ,

where  $\Lambda(x) := \mathbb{E}(\nabla\mathcal{L}_{\gamma_1}(x) - \nabla\mathcal{L}(x))^{\otimes 3}$ , and  $\overline{\mathcal{T}}$  denotes the symmetrization of tensor  $\mathcal{T}$ , i.e.,  $\overline{\mathcal{T}}_{ijk} = \frac{1}{6} \sum_{i',j',k'} \mathcal{T}_{i'j'k'}$ , where  $i', j', k'$  is a permutation of  $i, j, k$ .

*Proof.* Recall  $\Delta(x) = -\frac{\eta}{l}\nabla\mathcal{L}_{\bar{\gamma}}(x)$ , where  $\mathcal{L}_{\bar{\gamma}}(x) = \frac{1+\sqrt{2l-1}}{2}\mathcal{L}_{\gamma_1}(x) + \frac{1-\sqrt{2l-1}}{2}\mathcal{L}_{\gamma_2}(x)$ . Taking expectations, (i) and (ii) are immediate. Note  $|\Delta(x)| = O(l^{-0.5})$ , (iv) also holds.

Below we show (iii). For convenience, we denote  $\sqrt{2l-1}$  by  $c$ ,  $\nabla = \nabla\mathcal{L}(x)$ ,  $\tilde{\nabla}_i = \nabla\mathcal{L}_{\gamma_i}(x) - \nabla\mathcal{L}(x)$ , for  $i = 1, 2$  and  $\tilde{\nabla} = \frac{1+c}{2}\tilde{\nabla}_1 + \frac{1-c}{2}\tilde{\nabla}_2 = \nabla\mathcal{L}_{\gamma}(x) - \nabla\mathcal{L}(x)$ . We have

$$\begin{aligned} \mathbb{E}\frac{l^3}{\eta^3}\Delta(x)^{\otimes 3} &= \mathbb{E}(\tilde{\nabla} + \nabla)^{\otimes 3} \\ &= \mathbb{E}\tilde{\nabla}^{\otimes 3} + 3\mathbb{E}\overline{\tilde{\nabla} \otimes \tilde{\nabla} \otimes \nabla} + \nabla^{\otimes 3} \quad (\mathbb{E}\tilde{\nabla} = 0) \\ &= \mathbb{E}\tilde{\nabla}^{\otimes 3} + 3\mathbb{E}\overline{\Sigma \otimes \nabla} + \nabla^{\otimes 3} \\ &= \frac{3l-1}{2}\Lambda(x) + 3\mathbb{E}\overline{\Sigma \otimes \nabla} + \nabla^{\otimes 3}, \end{aligned}$$

where the last step is because

$$\begin{aligned} \mathbb{E}\tilde{\nabla}^{\otimes 3}(x) &= \mathbb{E}\left(\frac{1+c}{2}\tilde{\nabla}_1 + \frac{1-c}{2}\tilde{\nabla}_2\right)^{\otimes 3}(x) \\ &= \left[\left(\frac{1+c}{2}\right)^3 + \left(\frac{1-c}{2}\right)^3\right]\mathbb{E}(\nabla\mathcal{L}_{\gamma_1}(x) - \nabla\mathcal{L}(x))^{\otimes 3} \\ &= \left[\left(\frac{1+c}{2}\right)^3 + \left(\frac{1-c}{2}\right)^3\right]\Lambda(x) \\ &= \frac{3l-1}{2}\Lambda(x). \end{aligned}$$

$\square$

### C. Auxiliary results for the proof of Thm. 4.1

**Lemma C.1.** *Let  $\alpha \geq 1$ , there exists a  $K \in G$ , independent of  $l$ , such that*

$$\mathbb{E} \prod_{j=1}^{\alpha} |\tilde{\Delta}_{(i_j)}| \leq K(x) l^{-\frac{\alpha}{2}}.$$

where  $i_j \in \{1, \dots, d\}$  and  $C > 0$  is independent of  $l$ .

*Proof.* We have

$$\begin{aligned} \mathbb{E}|\tilde{\Delta}(x)|^{\alpha} &\leq 2^{\alpha-1} \mathbb{E} \left| \int_0^{\frac{\eta}{l}} \nabla \mathcal{L}(X_s^{x,0}) ds \right|^{\alpha} + 2^{\alpha-1} \mathbb{E} \left| \int_0^{\frac{\eta}{l}} \Sigma^{0.5}(X_s^{x,0}) dW_s \right|^{\alpha} \\ &\leq 2^{\alpha-1} \left( \frac{\eta}{l} \right)^{\alpha} \int_0^{\frac{\eta}{l}} \mathbb{E}|\nabla \mathcal{L}(X_s^{x,0})|^{\alpha} ds + 2^{\alpha-1} \left| \int_0^{\frac{\eta}{l}} \Sigma^{0.5}(X_s^{x,0}) dW_s \right|^{\alpha} \end{aligned}$$

Using Cauchy-Schwarz inequality, Itô's isometry, we get

$$\begin{aligned} \mathbb{E} \left| \int_0^{\frac{\eta}{l}} \sigma(X_s^{x,0}) dW_s \right|^{\alpha} &\leq \left( \mathbb{E} \left| \int_0^{\frac{\eta}{l}} \sigma(X_s^{x,0}) dW_s \right|^{2\alpha} \right)^{1/2} \\ &\leq C \left( \frac{\eta}{l} \right)^{\alpha-1/2} \left( \int_0^{\frac{\eta}{l}} \mathbb{E}|\sigma(X_s^{x,0})|^{2\alpha} ds \right)^{1/2} \\ &= O(l^{-\alpha/2}) \end{aligned}$$

where  $C$  depends only on  $\alpha$ . Now, using the linear growth condition (4.1 (ii)) and the moment estimates in Theorem 19 in (Li et al., 2019a), we obtain the result.  $\square$

We prove the following Itô-Taylor expansion, which is slightly different from Lemma 28 in (Li et al., 2019a).

**Lemma C.2.** *Let  $\psi : \mathbb{R}^d \rightarrow \mathbb{R}$  be a sufficiently smooth function.*

*Suppose that  $b, \sigma \in G^3$ , and  $X_t^{x,0}$  is the solution of the following SDE, with  $X_0^{x,0} = x$ .*

$$dX_t = b(X_t)dt + \sigma(X_t)dW_t.$$

*Then we have*

$$\mathbb{E}\psi(X_{\eta}^{x,0}) = \psi(x) + \eta b(x)^{\top} \nabla \psi(x) + \eta \text{Tr} [\nabla^2 \psi \cdot \sigma^2](x) + \mathcal{O}(\eta^2).$$

*That is, there exists some function  $K \in G$  such that*

$$|\mathbb{E}\psi(X_{\eta}^{x,0}) - \psi(x) - \eta b(x)^{\top} \nabla \psi(x) - \eta \text{Tr} [\nabla^2 \psi \cdot \sigma^2](x)| \leq K(x)\eta^2.$$

*Proof.* We define operator  $A_{1,\epsilon}\psi := b^{\top} \nabla \psi$ ,  $A_{2,\epsilon}\psi := \frac{1}{2} \text{Tr} [\nabla^2 \psi \cdot \sigma^2]$ .

Using Itô's formula, we have

$$\mathbb{E}\psi(X_{\eta}^{x,0}) = \psi(x) + \int_0^{\eta} \mathbb{E}A_{1,\epsilon}\psi(X_s^{x,0}) ds + \int_0^{\eta} \mathbb{E}A_{2,\epsilon}\psi(X_s^{x,0}) ds$$

By further application of the above formula to  $\mathbb{E}A_{1,\epsilon}\psi$  and  $\mathbb{E}A_{2,\epsilon}\psi$ , we have

$$\begin{aligned} \mathbb{E}\psi(X_{\eta}^{x,0}) &= \psi(x) + \eta A_{1,\epsilon}\psi(x) + \eta A_{2,\epsilon}\psi(x) \\ &\quad + \int_0^{\eta} \int_0^s \mathbb{E}((A_{1,\epsilon} + A_{2,\epsilon})(A_{1,\epsilon} + A_{2,\epsilon}))\psi(X_v^{x,0}) dv ds \end{aligned}$$

Taking expectations of the above, it remains to show that each of the terms is  $\mathcal{O}(\eta^2)$ . This follows immediately from the assumption that  $b, \sigma \in G^3$  and  $\psi \in G^4$ . Indeed, observe that all the integrands have at most 3 derivatives in  $b_0, b_1, \sigma_0$  and 4 derivatives in  $\psi$ , which by our assumptions all belong to  $G$ . Thus, the expectation of each integrand is bounded by  $\kappa_1(1 + \sup_{t \in [0, \eta]} \mathbb{E}|X_t^{x, 0}|^{2\kappa_2})$  for some  $\kappa_1, \kappa_2$ , which by Theorem 19 in (Li et al., 2019a) must be finite. Thus, the expectations of the other integrals are  $\mathcal{O}(\eta^2)$  by the polynomial growth assumption and moment estimates in Theorem 19 in (Li et al., 2019a).  $\square$

We also prove a general moment estimate for the SVAG iterations Equation (3).

**Lemma C.3.** *Let  $\{x_k : k \geq 0\}$  be the generalized SVAG iterations defined in Equation (3). Suppose*

$$|\nabla \mathcal{L}_\gamma(x)| \leq L_\gamma(1 + |x|), \quad \forall x \in \mathbb{R}^d, \gamma$$

for some random variable  $L_\gamma > 0$  with all moments bounded, i.e.,  $\mathbb{E}L_\gamma^k < \infty$ , for  $k \in \mathbb{N}$ . Then, for fixed  $T > 0$  and any  $m \geq 1$ ,  $\mathbb{E}|x_k|^{2m}$  exists and is uniformly bounded in  $l$  and  $k = 0, \dots, N \equiv \lfloor lT/\eta \rfloor$ .

*Proof.* Recall that  $\nabla \mathcal{L}_{\bar{\gamma}_k}^l(x) = \frac{1+\sqrt{2l-1}}{2} \nabla \mathcal{L}_{\gamma_{k,1}}(x) + \frac{1-\sqrt{2l-1}}{2} \nabla \mathcal{L}_{\gamma_{k,2}}(x)$ , thus there exists random variable  $L'_{\bar{\gamma}}$  with all moments bounded and  $|\nabla \mathcal{L}_{\bar{\gamma}_k}^l(x)|^2 \leq l(L'_{\bar{\gamma}})^2(1 + |x|^2)$ . We further define  $L := \mathbb{E}L_\gamma$ , and thus  $|\langle \mathbb{E}\nabla \mathcal{L}_{\bar{\gamma}_k}^l(x_k), x_k \rangle| \leq 2L(1 + |x_k|^2)$ .

For each  $k \geq 0$ , we have

$$\begin{aligned} |x_{k+1}|^{2m} &\leq (1 + |x_{k+1}^2|)^m = \left| 1 + |x_k|^2 - 2\frac{\eta}{l} \langle \nabla \mathcal{L}_{\bar{\gamma}_k}^l(x_k), x_k \rangle + \frac{\eta^2}{l^2} |\nabla \mathcal{L}_{\bar{\gamma}_k}^l(x_k)|^2 \right|^m \\ &= (1 + |x_k|)^{2m} - 2m\frac{\eta}{l} \langle \nabla \mathcal{L}_{\bar{\gamma}_k}^l(x_k), x_k \rangle (1 + |x_k|^2)^{m-1} + \frac{1}{l} \cdot O((|x_k|^2 + 1)^m) \end{aligned}$$

Hence, if we let  $a_k := \mathbb{E}(1 + |x_k|^2)^m$ , we have

$$a_{k+1} = a_{k+1} - 2m\frac{\eta}{l} \langle \mathbb{E}\nabla \mathcal{L}_{\bar{\gamma}_k}^l(x_k), x_k \rangle (1 + |x_k|^2)^{m-1} + \frac{1}{l} \cdot O((|x_k|^2 + 1)^m) \leq (1 + \frac{C}{l})a_k$$

where  $C > 0$  are independent of  $l$  and  $k$ , which immediately implies, for all  $k = 0, \dots, \lfloor \frac{lT}{\eta} \rfloor$ ,

$$a_k \leq (1 + C/l)^k a_0 \leq (1 + C/l)^{lT/\eta} a_0 \leq e^{C \frac{lT}{\eta}} a_0.$$

$\square$

## D. Omitted proofs in Section 6

In this section, we provide the missing proofs in Section 6, including Theorem 6.5, Theorem 6.6 and the counterpart of Theorem 6.2 between 1st order SDE (2) and 2nd order SDE (16). We also provide the derivation of properties for scale invariant functions in Appendix D.4.

### D.1. Proof of Theorem 6.6

*Proof of Theorem 6.6.* Similar to Equation (14), we have

$$(2 - \kappa\eta\lambda)\lambda R_\infty^{\kappa B} = \kappa\eta(G_\infty^{\kappa B} + N_\infty^{\kappa B}), \quad (21)$$

$$(2 - \eta\lambda)\lambda R_\infty^B = \eta(G_\infty^B + N_\infty^B), \quad (22)$$

Thus combining (21), (22) and (11), we have

$$\kappa(G_\infty^{\kappa B} + N_\infty^{\kappa B}) = (2 - \kappa\eta\lambda)\frac{\lambda}{\eta} R_\infty^{\kappa B} \leq (2 - \eta\lambda)\frac{\lambda}{\eta} C R_\infty^B = C(N_\infty^B + G_\infty^B).$$

Applying (17) again, we have

$$\kappa G_\infty^B + N_\infty^B \leq C\kappa(G_\infty^{\kappa B} + N_\infty^{\kappa B}) \leq C^2(N_\infty^B + G_\infty^B).$$

Therefore we conclude that  $\kappa \leq C^2(1 + \frac{N_\infty^B}{G_\infty^B})$ .  $\square$

## D.2. Proof of Theorem 6.5

*Proof.* By (11), we have

$$CG_\infty^{\kappa B} + C\kappa N_\infty^{\kappa B} \geq G_\infty^B + N_\infty^B.$$

By (21), (22) and (11), we have

$$G_\infty^B + N_\infty^B = 2\lambda \frac{B}{\eta} R_\infty^B \geq \frac{2}{C} \lambda \frac{B}{\eta} R_\infty^{\kappa B} = \frac{\kappa}{C} (G_\infty^{\kappa B} + N_\infty^{\kappa B}). \quad (23)$$

Rearranging things, we have

$$N_\infty^{\kappa B} \geq \frac{\kappa - C^2}{\kappa(C^2 - 1)} G_\infty^{\kappa B} \geq \left(\frac{1}{C^2} - \frac{1}{\kappa}\right) G_\infty^{\kappa B}.$$

$\square$

## D.3. Necessary condition for $C$ -closeness between 1st order and 2nd order SDE approximation

Below we first recap the notion of 1st and 2nd order SDE approximation with weight decay (i.e.,  $\ell_2$  regularization). We first define  $\mathcal{L}'_\gamma(X) = \mathcal{L}_\gamma(X) + \frac{\lambda}{2}|X|^2$  and the SGD dynamics (24) can be written by

$$x_{k+1} = x_k - \eta \nabla \mathcal{L}'_\gamma(x_k) = x_k - \eta \nabla (\mathcal{L}_{\gamma_k}(X_t) + \frac{\lambda}{2}|X_t|^2) \quad (24)$$

Below we recap the 1st and 2nd order SDE approximation:

- 1st order SDE approximation:

$$dX_t = -\nabla(\mathcal{L}(X_t) + \frac{\lambda}{2}|X_t|^2)dt + \Sigma^{1/2}(X_t)dW_t \quad (25)$$

- 2nd order SDE approximation:

$$dX_t = -\nabla(\mathcal{L}'(X_t) + \frac{\eta}{4}|\nabla \mathcal{L}'(X_t)|^2)dt + \Sigma^{1/2}(X_t)dW_t \quad (26)$$

We first prove a useful lemma.

**Lemma D.1.** Suppose  $\mathcal{L}$  is scale invariant, then for any  $X \in \mathbb{R}^d$ ,  $X \neq 0$ ,

$$X^\top \nabla^2 \mathcal{L}(X) \nabla \mathcal{L}(X) = \frac{1}{2} X^\top \nabla(\|\nabla \mathcal{L}\|_2^2) = -\|\nabla \mathcal{L}(X)\|_2^2.$$

*Proof.* By chain rule, we have

$$\begin{aligned} & X^\top \nabla(\|\nabla \mathcal{L}\|_2^2) \\ &= \lim_{t \rightarrow 0} \frac{\|\nabla \mathcal{L}((1+t)X)\|_2^2 - \|\nabla \mathcal{L}(X)\|_2^2}{t} \\ &= \lim_{t \rightarrow 0} \frac{(1+t)^{-2} - 1}{t} \|\nabla \mathcal{L}(X)\|_2^2 \quad (\text{by scale invariance}) \\ &= -2 \|\nabla \mathcal{L}(X)\|_2^2 \end{aligned}$$

$\square$

**Definition D.2** ( $C$ -closeness). We use  $\bar{R}'_\infty := \lim_{t \rightarrow \infty} E|X_t|^2$ ,  $\bar{G}'_\infty := \lim_{t \rightarrow \infty} \mathbb{E}|\nabla \mathcal{L}(X_t)|^2$ ,  $\bar{N}'_\infty := \lim_{t \rightarrow \infty} \mathbb{E}[\text{Tr}[\Sigma(X_t)]]$  to denote the limiting squared norm, gradient norm and trace of covariance for SDE (26). (We assume both  $X_t$  converge to their equilibrium so the limits exist). We say the two equilibriums of 1st order SDE approximation (25) and 2nd order SDE approximation (28) are  $C$ -close to each other iff

$$\frac{1}{C} \leq \frac{\bar{R}_\infty}{\bar{R}'_\infty}, \frac{\bar{G}_\infty}{\bar{G}'_\infty}, \frac{\bar{N}_\infty}{\bar{N}'_\infty} \leq C. \quad (27)$$

The following theorem is an analog of Theorem 6.2.

**Theorem D.3.** *If the equilibriums of (25) and (26) exist and are  $C$ -close for some  $C > 0$ , then*

$$\eta \leq \frac{\bar{N}_\infty}{\bar{G}_\infty} \left( C^2 \left( 1 + \frac{\eta\lambda}{2} \right) - 1 \right) \approx \frac{\bar{N}_\infty}{\bar{G}_\infty} (C^2 - 1),$$

where  $\lambda$  is usually of scale  $10^{-4}$  in practice and thus can be omitted when calculating upper bound.

*Proof.* Since  $\mathcal{L}$  is scale-invariant, so  $\nabla \mathcal{L}(X)^\top X = 0$ , which implies  $|\nabla \mathcal{L}'(X)|^2 = |\nabla \mathcal{L}(X)|^2 + \lambda^2 |X|^2$ . Plug in  $\mathcal{L}'$ , we have

$$dX_t = - \left( \nabla \mathcal{L}(X_t) + \frac{\eta}{2} \nabla^2 \mathcal{L}(X_t) \nabla \mathcal{L}(X_t) \right) dt + \Sigma^{1/2}(X_t) dW_t - \lambda \left( 1 + \frac{\eta\lambda}{2} \right) X_t dt. \quad (28)$$

Applying Ito' lemma, we have

$$\begin{aligned} d|X_t|^2 &= 2 \langle X_t, dX_t \rangle + \langle dX_t, dX_t \rangle \\ &= -2\lambda \left( 1 + \frac{\eta\lambda}{2} \right) |X_t|^2 dt - \eta \langle X_t, \nabla^2 \mathcal{L}(X_t) \nabla \mathcal{L}(X_t) \rangle dt + 2 \langle X_t, \Sigma^{1/2}(X_t) dW_t \rangle - 2 \langle X_t, \nabla \mathcal{L}(X_t) \rangle dt \\ &\quad + \text{Tr}[\Sigma(X_t)] dt \\ &= -2\lambda \left( 1 + \frac{\eta\lambda}{2} \right) |X_t|^2 dt - \eta \langle X_t, \nabla^2 \mathcal{L}(X_t) \nabla \mathcal{L}(X_t) \rangle dt + \text{Tr}[\Sigma(X_t)] dt \quad (\text{by Corollary D.7}) \\ &= -2\lambda \left( 1 + \frac{\eta\lambda}{2} \right) |X_t|^2 dt + (\text{Tr}[\Sigma(X_t)] + \eta |\nabla \mathcal{L}(X_t)|^2) dt \quad (\text{by Lemma D.1}) \end{aligned} \quad (29)$$

Thus

$$\frac{d\mathbb{E}[|X_t|^2]}{dt} = -2\lambda \left( 1 + \frac{\eta\lambda}{2} \right) \mathbb{E}[|X_t|^2] + \mathbb{E}[\text{Tr}[\Sigma(X_t)] + \eta |\nabla \mathcal{L}(X_t)|^2]. \quad (30)$$

Suppose  $X_t$  is samples from the equilibrium, we have  $\frac{d\mathbb{E}[|X_t|^2]}{dt} = 0$  and

$$(2 + \eta\lambda) \lambda \bar{R}'_\infty = \eta \bar{G}'_\infty + \bar{N}'_\infty. \quad (31)$$

If we compare Equation (31) to Equations (14) and (15) (we recap them below), it's quite clear 2nd order is much closer to SGD in terms of the relationship between  $R_\infty$ ,  $G_\infty$  and  $N_\infty$ . Thus 1st and 2nd order SDE approximation won't be  $C$ -close if  $\frac{\bar{N}_\infty}{\bar{G}_\infty}$  is larger than some constant for the exact same reason that 1st SDE is not  $C$ -close to SGD.

$$(2 - \eta\lambda) \lambda R_\infty = \eta G_\infty + \eta N_\infty, \quad (14)$$

$$2\lambda \bar{R}_\infty = \quad + \bar{N}_\infty. \quad (15)$$

□

In detail, by combining (31), (15) and (27), we have

$$\eta \bar{G}'_\infty + \bar{N}'_\infty = (2 + \eta\lambda) \lambda \bar{R}'_\infty \leq (2 + \eta\lambda) \lambda C \bar{R}_\infty = (1 + \frac{\eta\lambda}{2}) C \bar{N}_\infty.$$

Applying (27) again, we have

$$\eta \bar{G}_\infty + \bar{N}_\infty \leq C(\eta \bar{G}'_\infty + \bar{N}'_\infty) \leq C^2(1 + \frac{\eta\lambda}{2})\bar{N}_\infty,$$

which is  $\eta \leq (C^2(1 + \frac{\eta\lambda}{2}) - 1) \frac{\bar{N}_\infty}{\bar{G}_\infty}$ .

**Remark D.4.** *Kunin et al. (2020) derived a similar equation to Equation (29), which is the (28) in their paper. (As a corollary, they derive Equation (19)). However, they used normal chain rule as opposed to Ito's lemma in the first equality in (28) in their paper and thus omitted the contribution of the noise to the parameter norm, and reached the conclusion mistakenly that only expected gradient (but not noise covariance) affects the dynamics of the parameter norm.*

#### D.4. Properties of Scale Invariance Function

These properties are proved in (Arora et al., 2019b). We include them here for self-containedness.

**Definition D.5** (Scale Invariance). We say  $\mathcal{L} : \mathbb{R}^d \rightarrow \mathbb{R}$  is *scale invariant* iff  $\forall x \in \mathbb{R}^d, x \neq 0$  and  $\forall c > 0$ , it holds that

$$\mathcal{L}(cx) = \mathcal{L}(x).$$

We have the following two properties.

**Lemma D.6.** *If  $\mathcal{L}$  is scale invariant, then  $\forall x \in \mathbb{R}^d / \{0\}$ , we have*

1.  $\langle x, \nabla \mathcal{L}(x) \rangle = 0$ .
2.  $\forall c > 0, c \nabla \mathcal{L}(cx) = \nabla \mathcal{L}(x)$ .

*Proof.* For (1), by chain rule, we have  $\langle x, \nabla \mathcal{L}(x) \rangle = \lim_{t \rightarrow 0} \frac{\mathcal{L}((1+t)x) - \mathcal{L}(x)}{t} = 0$ .

For (2), for any  $v \in \mathbb{R}^d$ , again by chain rule, we have

$$\langle v, c \nabla \mathcal{L}(cx) \rangle = \langle cv, \nabla \mathcal{L}(cx) \rangle = \lim_{t \rightarrow 0} \frac{\mathcal{L}(cx + cvt) - \mathcal{L}(cx)}{t} = \lim_{t \rightarrow 0} \frac{\mathcal{L}(x + vt) - \mathcal{L}(x)}{t} = \langle v, \nabla \mathcal{L}(x) \rangle.$$

□

Suppose  $\mathcal{L}_\gamma$  is a random loss and is scale invariant for every  $\gamma$ , and we use  $\nabla \mathcal{L}(x)$  and  $\Sigma(x)$  to denote the expectation and covariance of gradient, then for any  $x \in \mathbb{R}^d / \{0\}$ , we have the following corollary:

**Corollary D.7.**  $\langle x, \nabla \mathcal{L}(x) \rangle = 0, x^\top \Sigma(x) x = 0$ .

## E. Experiments

We use the models from Github Repository: <https://github.com/bearpaw/pytorch-classification>. For VGG and PreResNet, unless noted otherwise, we modified the model following Appendix C of (Li & Arora, 2020) so that the network is scale invariant, e.g., fixing the last layer. Such modification doesn't lead to change in performance, as shown in (Hoffer et al., 2018). We use Weights & Biases to manage our experiments (Biewald, 2020).

### E.1. Further Verification of SVAG

We verify that SVAG converges for different architectures (including ones without normalization), learning rate schedules, and datasets. We further conclude that for most the standard settings we consider (excluding the use of large batch size in Figures 1 and 13 and GroupNorm on CIFAR-100 in Figure 12), SVAG with large  $l$  achieves similar performance to SGD, i.e. SVAG with  $l = 1$ .

#### E.1.1. FURTHER VERIFICATION OF SVAG ON MORE ARCHITECTURES ON CIFAR-10

For all CIFAR-10 experiments in this subsection, there are 320 epochs with initial LR  $\eta = 0.8$  and 2 LR decays by a factor of 0.1 at epochs 160 and 240 and we use weight decay with  $\lambda = 5e-4$  and batch size  $B = 128$ .

In Figure 7, we demonstrate that SVAG converges and closely follows SGD for PreResNet32 with BatchNorm (left), PreResNet32 (4x) with BatchNorm (middle) and PreResNet32 with GroupNorm (right).

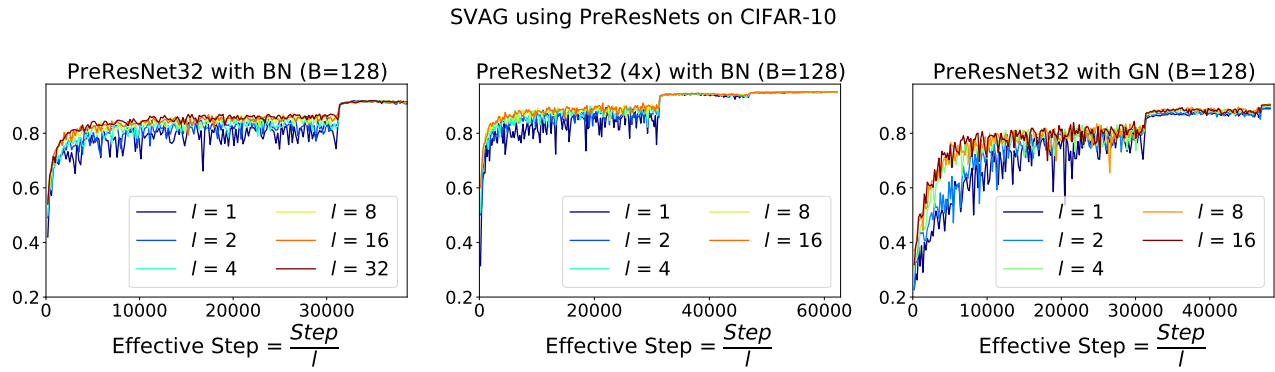


Figure 7. Validation accuracy for PreResNet32 with BatchNorm (left), PreResNet32 (4x) with BatchNorm (middle) and PreResNet32 with GroupNorm (right) during training on CIFAR-10. SVAG converges and closely follows the SGD trajectory in all three cases. Since SVAG takes  $l$  smaller steps to simulate the continuous dynamics in  $\eta$  time, we plot accuracy against “effective steps” defined as  $\frac{\# \text{steps}}{l}$ .

In Figure 8, we demonstrate that SVAG converges and closely follows SGD for VGG16 without Normalization (left), VGG16 with BatchNorm (middle) and VGG16 with GroupNorm (right).

#### E.1.2. FURTHER VERIFICATION OF SVAG ON MORE COMPLEX LR SCHEDULES

We verify that SVAG converges and closely follows the SGD trajectory for networks trained with more complex learning rate schedules. In Figure 10, we use the triangle (i.e., cyclical) learning rate schedule proposed in (Smith, 2017), visualized in Figure 9. We implement the schedule over 320 epochs of training: we increase the initial learning rate 0.001 linearly to 0.8 over 80 epochs, decay the LR to 0.001 over the next 80 epochs, increase the LR to 0.4 over 80 epochs, and decay the LR to 0.001 over the remaining 80 epochs. As seen in Figure 10, SVAG converges to the SGD trajectory in this setting.

We further test SVAG on the cosine learning rate schedule proposed in (Loshchilov & Hutter, 2016) with  $\eta_{\max} = 0.8$  and  $\eta_{\min} = 0.001$  with total training budgets of 160 epochs. We visualize the schedule in Figure 9. In Figure 11, we see that SVAG converges and closely follows the SGD trajectory, suggesting the SDE (2) can model SGD trajectories with complex learning rate schedules as well.

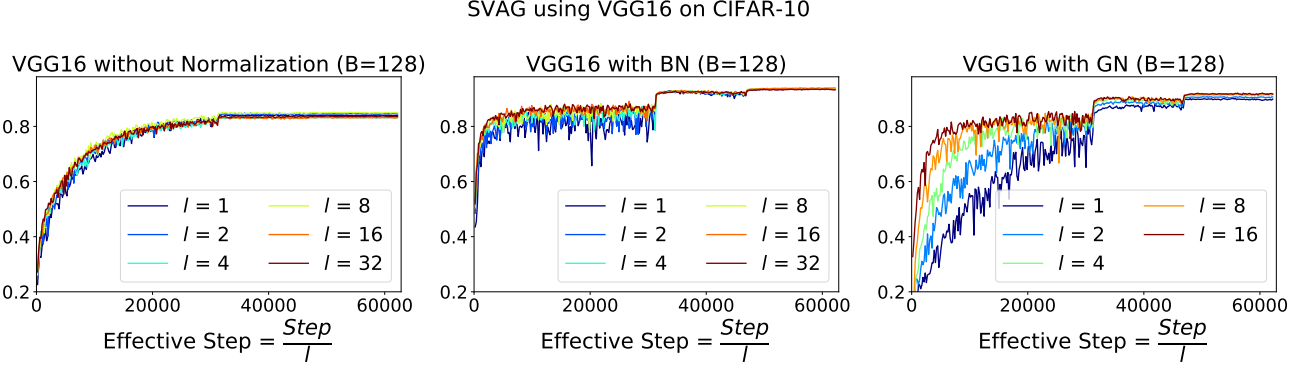


Figure 8. Validation accuracy for VGG16 without Normalization (left), VGG16 with BatchNorm (middle) and VGG16 with GroupNorm (right) during training on CIFAR-10. SVAG converges and closely follows the SGD trajectory in all three cases. Since SVAG takes  $l$  smaller steps to simulate the continuous dynamics in  $\eta$  time, we plot accuracy against “effective steps” defined as  $\frac{\#steps}{l}$ .

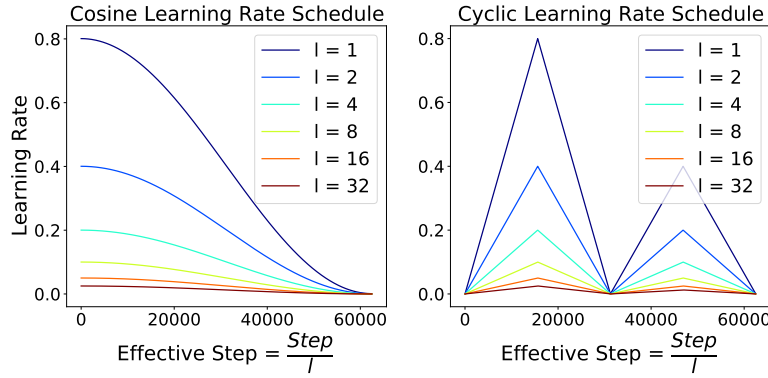


Figure 9. Cosine (left, (Loshchilov & Hutter, 2016)) and cyclic (right, (Smith, 2017)) learning rate schedules for different SVAG configurations, plotted against “effective steps” defined as  $\frac{\#steps}{l}$ .

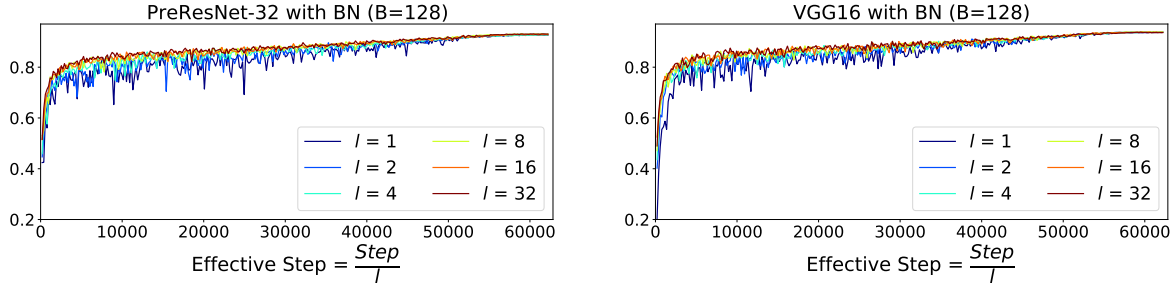


Figure 10. Validation accuracy for PreResNet-32 with  $B = 128$  (left) and VGG16 with  $B = 128$  (right) during training on CIFAR-10. We use the triangle LR schedule proposed in (Smith, 2017) with 80 epochs of increase to LR 0.8, 80 epochs of decay to 0, 80 epochs of increase to 0.4 and 80 epochs of decay to 0. The LR schedule is visualized in Figure 9. Since SVAG takes  $l$  smaller steps to simulate the continuous dynamics in  $\eta$  time, we plot accuracy against “effective steps” defined as  $\frac{\#steps}{l}$ .

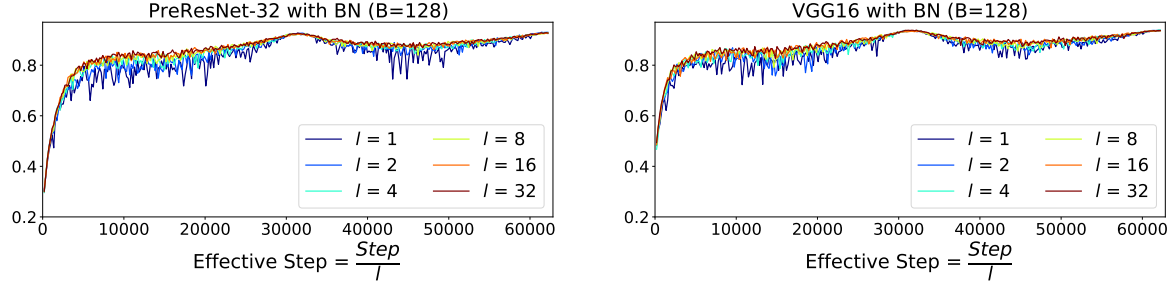


Figure 11. Validation accuracy for PreResNet-32 with  $B = 128$  (left) and VGG16 with  $B = 128$  (right) during training on CIFAR-10. We use the cosine LR schedule proposed in (Loshchilov & Hutter, 2016) starting with LR 0.8 and following the cosine curve until the LR becomes infinitesimally small. The LR schedule is visualized in Figure 9. Since SVAG takes  $l$  smaller steps to simulate the continuous dynamics in  $\eta$  time, we plot accuracy against “effective steps” defined as  $\frac{\# \text{steps}}{l}$ .

#### E.1.3. FURTHER VERIFICATION OF SVAG ON MORE DATASETS (CIFAR-100 AND SVHN)

We also verify that SVAG converges on the CIFAR-100 dataset. We set the learning rate to be 0.8 and decay it by a factor of 0.1 at epochs 160 and 240 with a total budget of 320 epochs. We use weight decay with  $\lambda = 5e-4$ . We observe that SVAG converges for computationally tractable value of  $l$  in Figure 12, but for both GN architectures, the SDE fails to approximate SGD training.

We also verify SVAG on the Street View House Numbers (SVHN) dataset (Netzer et al., 2011). We set the learning rate to 0.8 for batch size 128 and scale it according to LSR (Definition 5.1) for large batch training. We train for 240 epochs and decay the learning rate by a factor of 0.1 once at epoch 200. We use weight decay with  $\lambda = 5e-4$ .

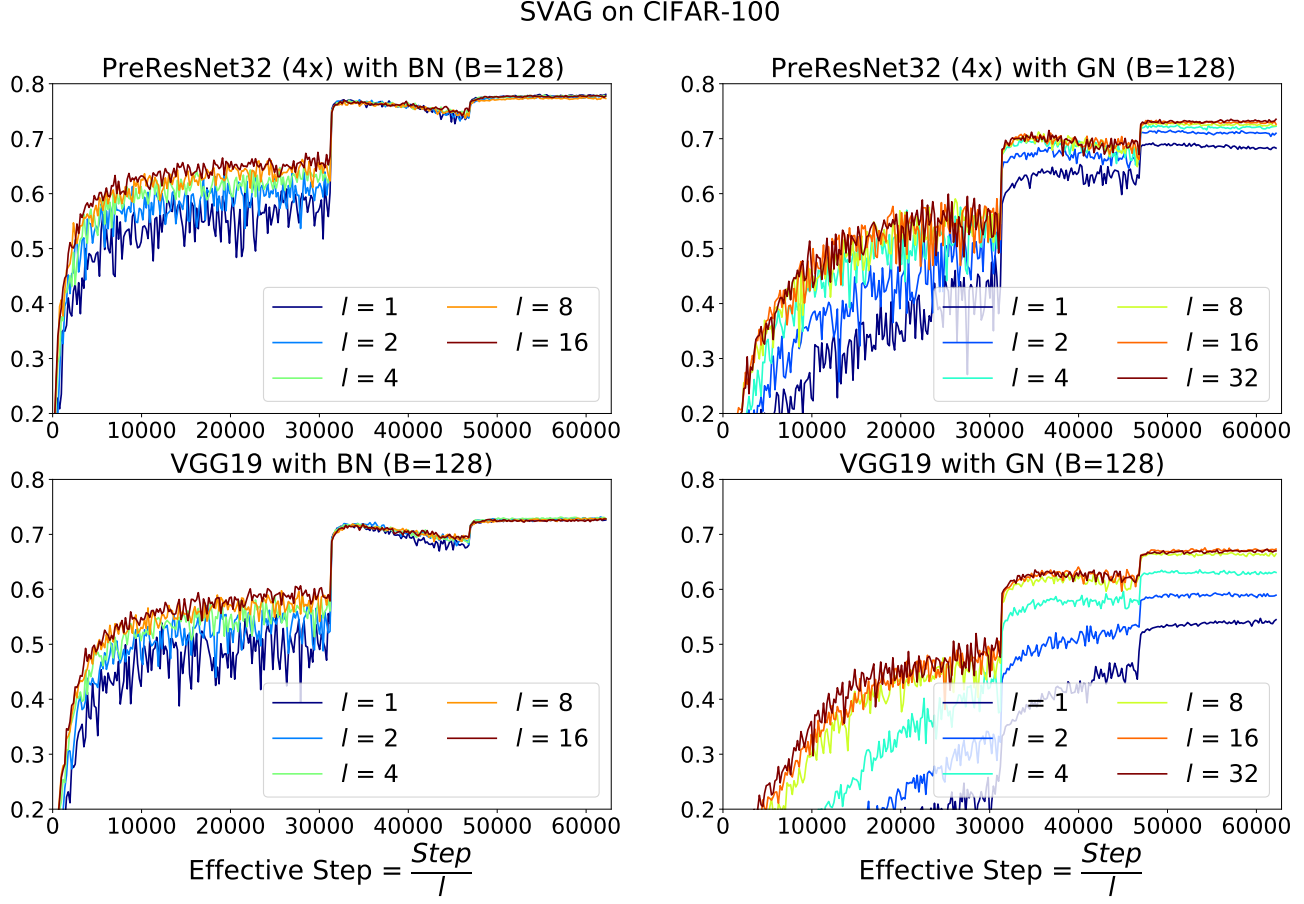


Figure 12. Validation accuracy for wider PreResNet-32 with  $B = 128$  using BN (top left) and GN (top right) and for VGG-19 with  $B = 128$  using BN (bottom left) and GN (bottom right) trained on CIFAR-100. We train for 320 epochs and decay the LR by 0.1 at epochs 160 and 240. Since SVAG takes  $l$  smaller steps to simulate the continuous dynamics in  $\eta$  time, we plot accuracy against “effective steps” defined as  $\frac{\# \text{steps}}{l}$ . Interestingly, we found the performance of BatchNorm out performs GroupNorm and the performance of the latter gets improved when using larger  $l$  for SVAG.

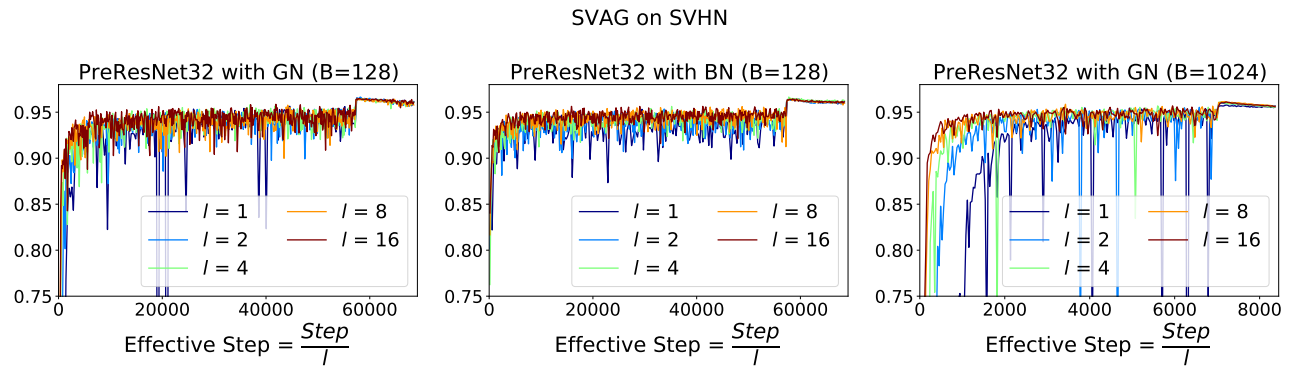


Figure 13. Validation accuracy for PreResNet-32 with  $B = 128$  using GN (left) and BN (center) and with  $B = 1024$  using GN trained on the SVHN dataset (Netzer et al., 2011). We train for 240 epochs and decay the LR by 0.1 at epoch 200. Since SVAG takes  $l$  smaller steps to simulate the continuous dynamics in  $\eta$  time, we plot accuracy against “effective steps” defined as  $\frac{\# \text{steps}}{l}$ .

## E.2. Further Verification of Necessary Condition for LSR

We further verify the necessary condition for LSR (Theorem 6.6) using different architectures and datasets. Figure 14 tests the condition for ResNet-32 and wider PreResNets trained on CIFAR-10. Although our theory requires strict scale-invariance, we find the condition to still be applicable to the standard ResNet architecture (He et al., 2016), ResNet32, likely because most of the network parameters are scale-invariant. Figure 15 tests the condition for wider PreResNets and VGG-19 trained on CIFAR-100. We require the wider PreResNet to achieve reasonable test error, but we note that the larger model made it difficult to straightforwardly train with a larger batch size.

In Figure 14 and Figure 6,  $G_t$  and  $N_t$  are the empirical estimations of  $G_\infty$  and  $N_\infty$  taken after reaching equilibrium in the second to last phase (before the final LR decay), where the number of samples (batches) is equal to  $\max(200, 50000/B)$ , and  $B$  is the batch size.

Per the approximated version of Theorem 6.6, i.e.,  $B^* = \kappa B \lesssim C^2 B N_\infty^B / G_\infty^B$ , we use baseline runs with different batch sizes  $B$  to report the maximal and minimal predicted critical batch size, defined as the x-coordinate of the intersection of the threshold ( $G_t/N_t = C^2$ ) with the green and blue lines, respectively. Both the green and blue line have slope 1, and thus the x-coordinate of intersection,  $B^*$ , is the solution of the following equation,

$$\frac{B^*}{B} = \frac{G_t^{B^*}/N_t^{B^*}}{G_t^B/N_t^B}, \text{ where } G_t^{B^*}/N_t^{B^*} = C^2.$$

For all settings, we choose a threshold of  $C^2 = 2$ , and consider LSR to fail if the final test error exceeds the lowest achieved test error by more than 20% of its value, marked by the red region on the plot. Surprisingly, it turns out the condition in Theorem 6.6 is not only necessary, but also close to sufficient.

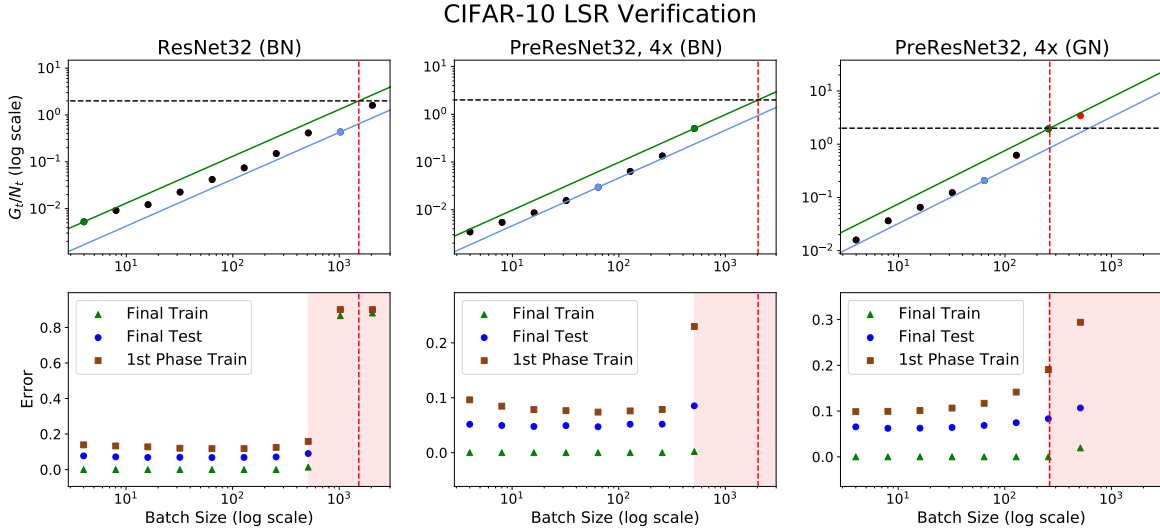


Figure 14. Further verification for our theory on predicting the failure of Linear Scaling Rule. We test if the condition applies to different architectures trained on CIFAR-10. All three settings use the same LR schedule, LR = 0.8 initially and is decayed by 0.1 at epoch 250 with 300 epochs total budget. We measure  $G_t$  and  $N_t$  by averaging their values over the last 50 epochs of the first phase (i.e., from epoch 200 to 250).

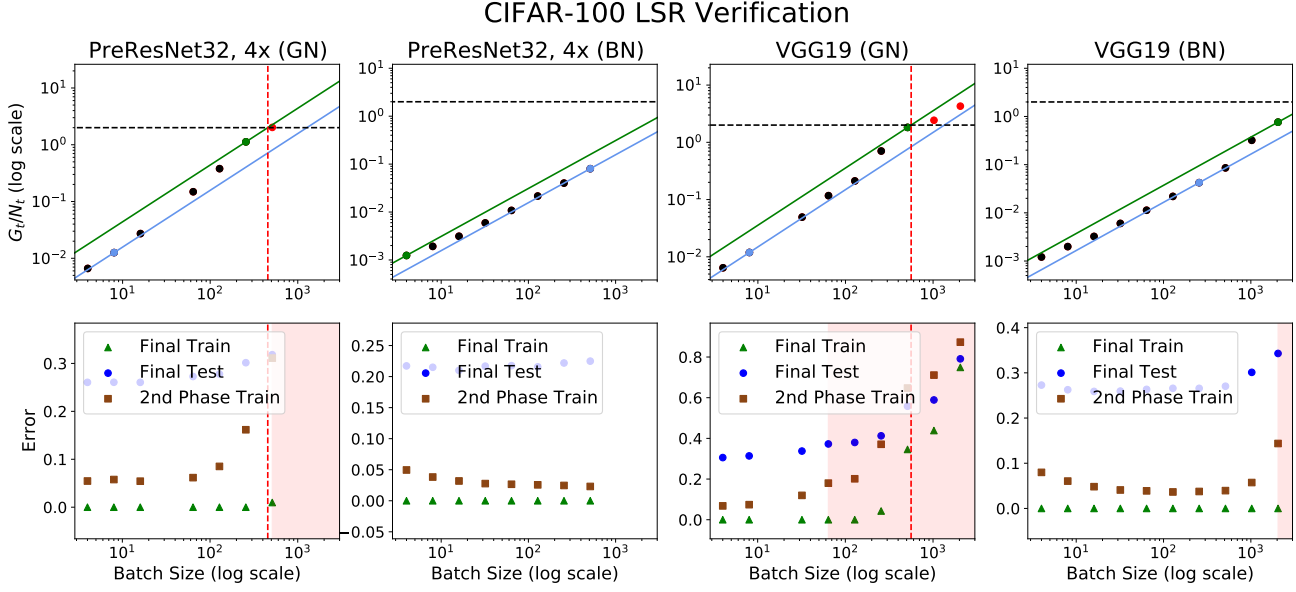


Figure 15. Further verification for our theory on predicting the failure of Linear Scaling Rule. We test if the condition applies to different architectures trained on CIFAR-100. All four settings use the same LR schedule, LR= 0.8 initially and is decayed by 0.1 at epoch 80 and again at epoch 250 with 300 epochs total budget. We measure  $G_t$  and  $N_t$  by averaging their values over the last 50 epochs of the second phase (i.e., from epoch 200 to 250).

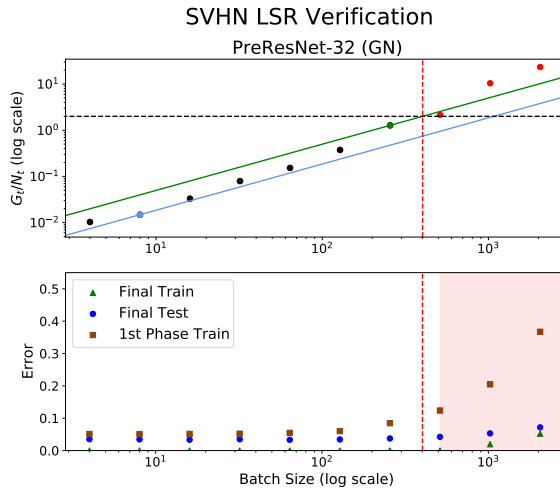


Figure 16. Further verification for our theory on predicting the failure of Linear Scaling Rule. We test if the condition applies to PreResNet-32 with GN trained on SVHN (Netzer et al., 2011). LR= 0.8 initially and is decayed by 0.1 at epoch 100 with 120 epochs total budget. We measure  $G_t$  and  $N_t$  by averaging their values over the last 20 epochs of the second phase (i.e., from epoch 80 to 100).

### E.3. Additional Experiments for NGD (Noisy Gradient Descent)

We provide further evidence that SGD and noisy gradient descent (NGD) have similar train and test curves in Figures 17, 18, and 19. To perform NGD, we replace the SGD noise by Gaussian noise with the same covariance as was done in (Wu et al., 2020). We note that each step of NGD requires computing the full-batch gradient over the entire dataset (in this case, done through gradient accumulation), which is much more costly than a single SGD step. Each figure took roughly 7 days on a single RTX 2080 GPU.

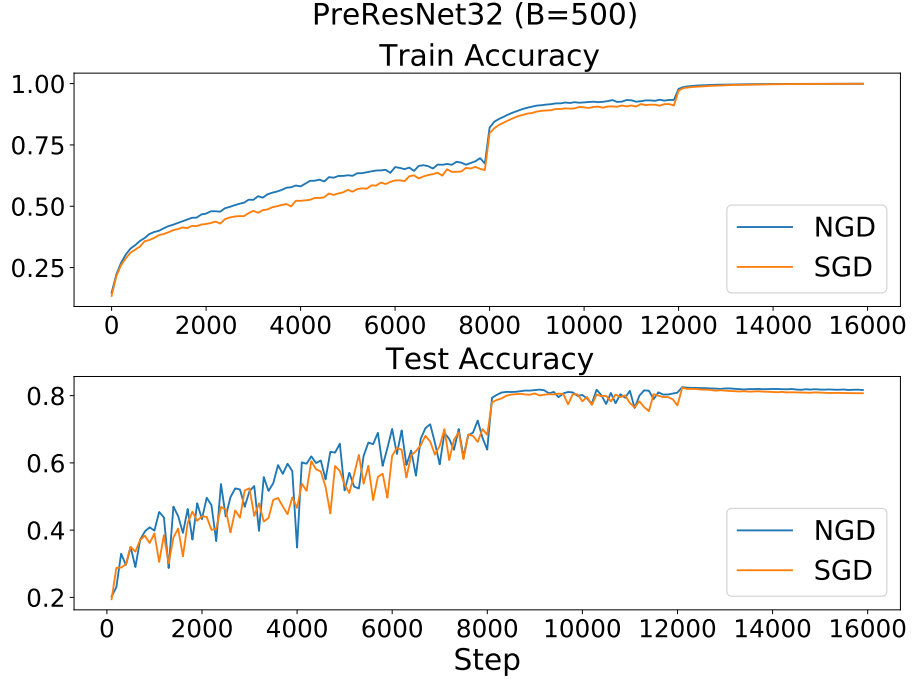


Figure 17. SGD and NGD with matching covariance have close train (top) and test (bottom) curves. The batch size for SGD is 500 and LR = 3.2 for both settings and decayed by 0.1 at step 8000. We smooth the training curve by dividing it into intervals of 100 steps and recording the average. For efficient sampling of Gaussian noise, we use GroupNorm instead of BatchNorm and turn off data augmentation. SGD and NGD achieve a maximum test accuracy of 82.3% and 82.5%, respectively

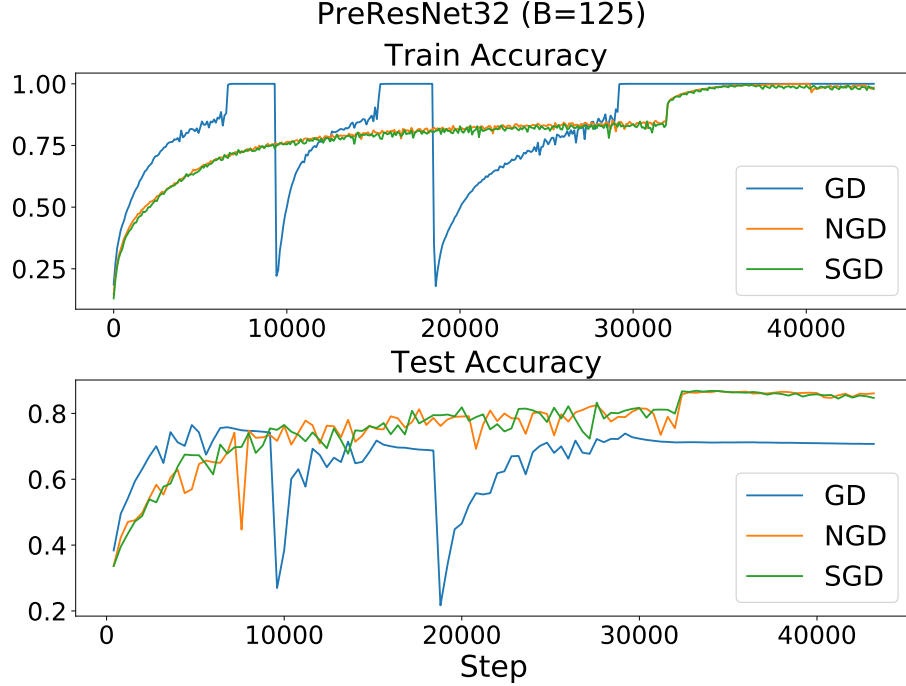


Figure 18. SGD and NGD with matching covariance have close train (top) and test (bottom) curves. The batch size for SGD is 125 and LR= 0.8 for all three settings and decayed by 0.1 at step 32000. We smooth the training curve by dividing it into intervals of 100 steps and recording the average. For efficient sampling of Gaussian noise, we use GroupNorm instead of BatchNorm and turn off data augmentation. GD achieves a maximum test accuracy of 76.5%, while SGD and NGD achieve 86.9% and 86.8%, respectively

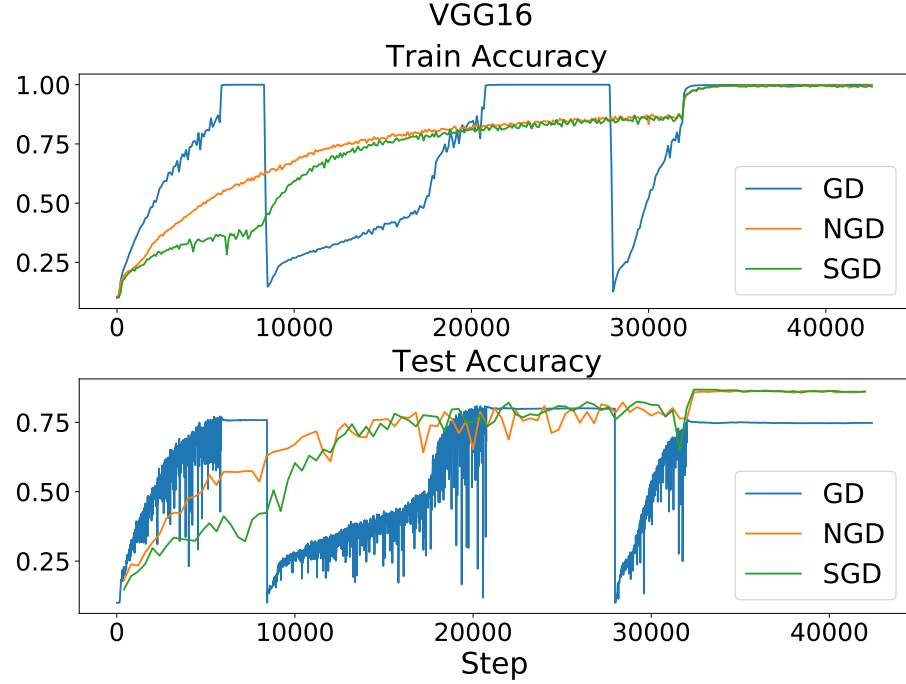


Figure 19. SGD and NGD with matching covariance have close train (top) and test (bottom) curves for VGG16. The batch size for SGD is 125 and LR= 0.8 for all three settings and decayed by 0.1 at step 32000. We smooth the training curve by dividing it into intervals of 100 steps and recording the average. For efficient sampling of Gaussian noise, we use GroupNorm instead of BatchNorm and turn off data augmentation. GD achieves a maximum test accuracy of 80.9%, while SGD and NGD achieve 86.8% and 86.5%, respectively

## F. Discussion on Non-Gaussian Noise

### F.1. LSR can hold when SDE approximation breaks

**Example F.1.** Let  $Z(t)$  be a 1-dimensional Levy process, e.g. poisson process, where  $Z(t)$  follows poisson distribution with parameter  $t$ . We assume the distribution of the gradient on single sampled data  $\gamma$ ,  $\nabla L_\gamma(x)$  is the same as  $Z(1)$  for any parameter  $x$ . For a i.i.d. sampled batch  $B$  of size  $B$  (with replacement), by the property of Levy Process,  $\nabla \mathcal{L}_B(x) := \frac{1}{B} \sum_{\gamma \in B} \nabla \mathcal{L}_\gamma(x) \stackrel{d}{=} \frac{Z(B)}{B}$ .

Thus performing SGD starting from  $x_0$  for  $\frac{T}{B}$  steps with LR  $B\eta$  and batch size  $B$ , the distribution of  $x_{\frac{T}{B}}$  is independent of  $B$ , i.e.,

$$\begin{aligned} x_k &= x_{k-1} - B\eta \nabla \mathcal{L}_B(x_{k-1}) \implies \\ x_{\frac{N}{B}} &\stackrel{d}{=} -\eta \underbrace{(Z(B) + Z(B) + \dots + Z(B))}_{\frac{T}{B} \text{ 's } Z(B)} \stackrel{d}{=} -\eta Z(T). \end{aligned}$$

### F.2. Heavy-tailed Noise and Unbounded Covariance

Simsekli et al. (2019) experimentally found that the distribution of the SGD noise appears to be heavy-tailed and proposed to model it with an  $\alpha$ -stable process. In detail, in Figure 1 of (Simsekli et al., 2019), they show that the histogram of the gradient noise computed with AlexNet on CIFAR-10 is more close to that of  $\alpha$ -stable random variables, instead of that of Gaussian random variables. However, a more recent paper (Xie et al., 2021) pointed out a fundamental limitation of methodology in (Simsekli et al., 2019): (Simsekli et al., 2019) made a hidden but very restrictive assumption that the noise of each parameter in the model is distributed identically. Moreover, their test (Theorem F.2) of the tail-index  $\alpha$  works only under this assumption. Thus the empirical measurement in (Simsekli et al., 2019) ( $\hat{\alpha} < 2$ ) doesn't exclude the possibility that that stochastic gradient noise follows a joint multivariate Gaussian.

**Theorem F.2.** (Mohammadi et al., 2015) Let  $\{X_i\}_{i=1}^K$  be a collection of i.i.d. random variables with  $X_1 \sim \mathcal{S}\alpha\mathcal{S}(\sigma)$  and  $K = K_1 \times K_2$ . Define  $Y_i := \sum_{j=1}^{K_1} X_{j+(i-1)K_1}$  for  $i \in \{1, \dots, K_2\}$ . Then the estimator

$$\widehat{\frac{1}{\alpha}} := \frac{1}{\log K_1} \left( \frac{1}{K_2} \sum_{i=1}^{K_2} \log |Y_i| - \frac{1}{K} \sum_{i=1}^K \log |X_i| \right). \quad (32)$$

converges to  $\frac{1}{\alpha}$  almost surely, as  $K_2 \rightarrow \infty$ . Here  $\mathcal{S}\alpha\mathcal{S}(\sigma)$  is the  $\alpha$ -stable distribution defined by  $X \sim \mathcal{S}\alpha\mathcal{S}(\sigma) \iff \mathbb{E}[\exp(iwX)] = \exp(-|\sigma w|^\alpha)$ .

We provide the following theoretical and experimental evidence on vision tasks to support the argument in (Xie et al., 2021) that it is reasonable to model the stochastic gradient noise by joint Gaussian random variables instead of  $\alpha$ -stable random variables even for finite learning rate. (Note SVAG (e.g., Figure 1) only shows that when LR becomes infinitesimally small, replacing the noise by Gaussian noise gets similar performance.)

1. In Figure 6, we find that the trace of covariance of noise is bounded and the empirical average doesn't grow with the number of samples/batches (this is not plotted in the current paper). However, an  $\alpha$ -stable random variable has unbounded variance for  $\alpha < 2$ .
2. In Figures 5, 18, 17, and 19, we show directly that replacing the stochastic gradient noise by Gaussian noise with the same covariance gets almost the train/test curve and the final performance.
3. Applying the test in Theorem F.2 on joint multivariate Gaussian random variables can yield an estimate ranged from 1 to 2 for the tail-index  $\alpha$ , but for Gaussian variables,  $\alpha = 2$ . (Theorem F.3)

Another recent work Zhang et al. (2019) also confirmed that the noise in stochastic gradient in ResNet50 on vision tasks is finite. However, they also found the noise for BERT on Wikipedia+Books dataset could be heavy-tailed: the empirical variance is not converging even with  $10^7$  samples. We left it as a future work to investigate how does SDE approximate SGD on those tasks or models with heavy-tailed noise.

**Theorem F.3.** Let  $K = K_1 \times K_2 = d \times m \times K_2$ , where  $K_1, K_2, d, m \in \mathbb{N}^+$ . Let  $\{X_i\}_{i=1}^K$  be a collection of random

variables where  $X_{(j-1)d+jd} \stackrel{i.i.d.}{\sim} N(0, \Sigma)$ , for each  $j \in \{1, \dots, mK_2\}$ . Then we have

$$\mathbb{E} \left[ \frac{1}{\log K_1} \left( \frac{1}{K_2} \sum_{i=1}^{K_2} \log |Y_i| - \frac{1}{K} \sum_{i=1}^K \log |X_i| \right) \right] = \frac{1}{2} \frac{\log m + \log \mathbf{1}^\top \Sigma \mathbf{1} - \frac{1}{d} \sum_{i=1}^d \log \Sigma_{ii}}{\log m + \log d}.$$

Specifically, when  $d = K_1$  and  $m = 1$ , taking  $\Sigma = \beta \mathbf{1} \mathbf{1}^\top + (1 - \beta)I$ , we have

$$\mathbb{E} \left[ \frac{1}{\log K_1} \left( \frac{1}{K_2} \sum_{i=1}^{K_2} \log |Y_i| - \frac{1}{K} \sum_{i=1}^K \log |X_i| \right) \right] = \frac{1}{2} \frac{\log(\beta d^2 + (1 - \beta)d)}{\log d},$$

and

$$\left\{ \frac{1}{2} \frac{\log(\beta d^2 + (1 - \beta)d)}{\log d} \mid \beta \in [0, 1] \right\} = \left[ \frac{1}{2}, 1 \right].$$

*Proof.*

$$\mathbb{E} \left[ \frac{1}{\log K_1} \left( \frac{1}{K_2} \sum_{i=1}^{K_2} \log |Y_i| - \frac{1}{K} \sum_{i=1}^K \log |X_i| \right) \right] = \mathbb{E} \left[ \frac{1}{\log K_1} \left( \log |Y_1| - \frac{1}{d} \sum_{i=1}^d \log |X_i| \right) \right]. \quad (33)$$

Note  $Y_1$  is gaussian with standard deviation  $\sqrt{\mathbf{1}^\top \Sigma \mathbf{1} \cdot m}$  and  $X_i$  is gaussian with standard deviation  $\sqrt{\Sigma_{ii}}$ . Thus  $\mathbb{E}[\log |Y_1| - \log |X_i|] = \log \sqrt{\mathbf{1}^\top \Sigma \mathbf{1} \cdot m} - \log \sqrt{\Sigma_{ii}}$ . Thus we have

$$\mathbb{E} \left[ \frac{1}{\log K_1} \left( \frac{1}{K_2} \sum_{i=1}^{K_2} \log |Y_i| - \frac{1}{K} \sum_{i=1}^K \log |X_i| \right) \right] \quad (34)$$

$$= \mathbb{E} \left[ \frac{1}{\log K_1} \left( \log |Y_1| - \frac{1}{d} \sum_{i=1}^d \log |X_i| \right) \right] \quad (35)$$

$$= \frac{1}{2} \frac{\log m + \log \mathbf{1}^\top \Sigma \mathbf{1} - \frac{1}{d} \sum_{i=1}^d \log \Sigma_{ii}}{\log m + \log d} \quad (36)$$

□